FUNCTIONAL ROLE OF RNA EDITING OF $CA_V1.3$ IQ DOMAIN

ZHAI JING

(B.Sc), Zhejiang University

A THESIS SUBMITTED

FOR THE DEGREE OF DOCTOR OF PHILOSOPHY

DEPARTMENT OF PHYSIOLOGY

NATIONAL UNIVERSITY OF SINGAPORE

2014

DECLARATION

I hereby declare that this thesis is my original work and it has been written by me in its entirety. I have duly acknowledged all the sources of information which have been used in the thesis.

This thesis has also not been submitted for any degree in any university previously

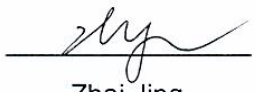

Zhai Jing

19th December 2014

Acknowledgements

I would like to express my gratitude towards Yong Loo Lin School of medicine NUS for sponsoring my graduate study. I am deeply indebted to my supervisor A/Prof Soong Tuck Wah for his guidance, encouragement and inspiration. I would like to thank A/Prof Lim Kah Leong and Dr. Yu Wei Ping for their advice and insightful comments as my Thesis Advice Committee. My sincere thanks also go to Dr. Yu Wei Ping for his advice in generation of $Ca_V1.3$ ECS knockout mice and providing us the Actin-CRE mice, Dr. Zhang Xiaodong for providing the THP2KI mice and Dr. Wong Peiyan for her kind help in phenotyping. I would also like to thank all my fellow labmates in Ion Channel and Transporter laboratory for their dedicated support throughout my PhD project. Last but not least, I would like to thank my family and friends for encouraging and supporting me all the time.

Table of Contents

List of Publications

1. Huang, H., Ng, C. Y., Yu, D., Zhai, J., Lam, Y., & Soong, T. W. Modest $Ca_V1.342$-Selective Inhibition by Compound 8 is β-subunit Dependent. Nat Commun, 2014, 5:4481

2. Zhai, J., Huang, H., Wong R.X., Wong P.Y., Yu W.P., & Soong T.W. RNA Editing of $Ca_V1.3$ Channel IQ domain Modulates Circadian Rhythm and Anxiety-like Behavior in Mice. (In preparation)

Abstracts

1. Zhai Jing and Soong Tuck Wah. RNA Editing in IQ Domain of $Ca_V1.3$ Channel. Models of Physiology and Disease Symposium, Singapore, 2012

2. Zhai Jing and Soong Tuck Wah. Modulation of IQ domain RNA editing under various physiological conditions. 8_{th} International Conference for Neurons and Brain Diseases, Singapore, 2013

3. J. Zhai, H. Huang, W.P. Yu and Soong Tuck Wah. Physiological Roles and Regulation of RNA Editing of IQ Domain of $Ca_V1.3$ Channel. Society for Neuroscience, San Diego, USA, 2013

Summary

Mutations in human *CACNA1D* gene encoding the $Ca_V1.3$ channel are associated with hearing loss, bradycardia and adrenal aldosterone-producing adenomas; while m*Cacan1d* null mice also showed mood disorder, besides bradycardia and deafness. Alterations in $Ca_V1.3$ function will therefore have neurological implications.

The IQ-domain of $Ca_V1.3$ undergoes A-to-I RNA editing to affect Ca^{2+}-dependent inactivation. Here, we showed that editing is influenced by physiological conditions: (i) RNA editing level increased in substantia nigra during aging and (ii) RNA editing was regulated in a circadian rhythmic fashion in the suprachasmatic nucleus.

We discovered the editing site complimentary sequence (ECS) essential for RNA editing by disruption of the hairpin structure using oligonucleotides. We then generated $Ca_V1.3$ $ECS^{-/-}$ mice where we demonstrated that RNA editing of the IQ domain was abolished in these mice. In our initial behavioural studies, we found that the $Ca_V1.3$ $ECS^{-/-}$ mice displayed anxiety like behavior and exhibited disruption in their circadian rhythm.

（150 words）

List of Tables

List of Figures

List of Abbreviation

5-HT2C	5-hydroxytryptamine (serotonin) receptor 2C
6-OHDA	6-hydroxydopamine
ADAR	adenosine deaminase acting on RNA
ADTRS	agonist-directed trafficking of receptor stimulus
AID	alpha interacting domain
AMPAR	α-amino-3-hydroxy-5-methyl-4-isoxazolepropionic acid receptor
ALS	amyotrophic lateral scerosis
AP	action potential
BAC	bacterial artificial chromosome
bp	base pairs (nucleotide)
CaM	Calmodulin
CaV	Voltage gated calcium channels
CDI	Calcium dependent inactivation
CaBP	Calcium-binding protein
Cb	Calbindin
cDNA	complementary deoxyribonucleic acid
CNS	central nervous system
Cldn14	Claudin 14
C-terminal	carboxyl-terminal
DA	dopaminergic
DCRD	distant C-terminal regulatory domain
DD	dark-dark
DHP	dihydropyridine

DMEM	Dulbecco’s Modified Eagle Medium
DNA	deoxyribonucleic acid
ECS	editing-site complementary sequence
EDTA	ethylenediamine tetraacetic acid
EGTA	ethyleneglycol tetraacetic acid
ER	endoplasmic reticulum
ES	embryonic stem
EZM	elevated zero maze
FBS	foetal bovine serum
GABA	gama-aminobutyric acid
GCaMP	eGFP-Calmodulin fusion protein
GFP	green fluorescence protein
GluR	glutamate receptor
HCN	Hyperpolarization-activated cyclic nucleotide-gated channel
HEK	human embryonic kidney cell line
HEPES	N-2-hyroxyethylpiperazine-N’2-ethanesulponic acid
IBa	Ba^{2+} current
ICa	Ca^{2+} current
IP	Immunoprecipitation
kb	kilo base pairs (nucleotide)
KO	knockout
Kv	voltage gated potasium channel
LD	light-dark
LF	long-form
mPTP	1-methyl-4-phenyl-1,2,3,6-tetrahydropyridine

mRNA	messenger ribonucleic acid
NSCaTE	N-terminal spatial Ca^{2+} transforming element
nt	nucleotides
N-terminal	amino-terminal
PCR	polymerase chain reaction
PCRD	proximal C-terminal regulatory domain
PD	Parkinson’s disease
PLA2-AA	phospholipase A2-arachidonic acid
PLC-PI	Phosphatidylinositol-specific phospholipase C
SAN	sinoatrial node
SCN	suprachiasmatic nucleus
SF	short-form
SNc	substantia nigra compacta
TPH2KI	tryptophan hydroxylase-2 knockin
UTR	untranslated region
VDI	voltage-dependent inactivation
WT	wild type

Chapter1

Introduction

1.1 L-type voltage gated calcium channel

The Ca_V channels are heteroligomeric transmembrane complexes composed of a pore-forming α1 subunit and auxiliary β, α2δ subunits (Catterall 2000). The L-type voltage gated calcium channel (Ca_V1) family comprises $Ca_V1.1$, $Ca_V1.2$, $Ca_V1.3$ and $Ca_V1.4$ channels. The strong depolarization, slow I_{Ba} inactivation and pharmacological sensitivity to dihydropyridines (DHPs) are the defining features of L-type calcium channel (Namkung et al. 2001).

1.2 Physiological roles of $Ca_V1.3$ calcium channel

The $Ca_V1.3$ calcium channel, one of the four L-type voltage-gated calcium channels, is a long-lasting calcium channel activated at low voltage responding to membrane depolarization for influx of Ca^{2+}. It is widely expressed in the central nervous system, cochlea and sino-atrial node (SAN) of the heart. These channels are also expressed in the endocrine system including the beta cells of the pancreas and chromaffin cells of the adrenal glands. It is known that $Ca_V1.3$ channels play an important role in gating low-threshold-activating Ca^{2+} currents that support neuroendocrine secretion of insulin (Marcantoni et al. 2007), neurotransmitter release associated with visual and auditory signal transmission (Zhang et al. 2005a, Zhang et al. 2006), neuronal pace-making activity in substantial nigra and suprachismatic nucleus (Chan et al. 2007, Peterson et al. 1999), and cardiac rhythmicity in cardiac sino-atrial node (Platzer et al. 2000). Besides, there are also growing evidences showing that $Ca_V1.3$ is involved in the modulation of

higher-order mental functions such as mood disorders (Perrine et al. 2010).

1.2.1 Physiological roles of $Ca_V1.3$ channels revealed in $\alpha1D^{-/-}$ mice

The α1D is the pore forming subunit of $Ca_V1.3$ channel (Figure 1). The known physiological roles of $Ca_V1.3$ were obtained from the characterizations of the $\alpha1D^{-/-}$ mice. One was generated by the Striessnig's group (Platzer et al. 2000), and another strain of $Ca_V1.3$-null mutant mice was from Hee-Sup Shin's group generated by gene-targeting method (Zhang et al. 2005c). Owing to their low-voltage activation threshold, $Ca_V1.3$ channels are responsible for significant inward current flow into the inner hair cells at the operating range for cochlear, for spontaneous firing in chromaffin cells and for pace making in SAN (Xu and Lipscombe 2001).

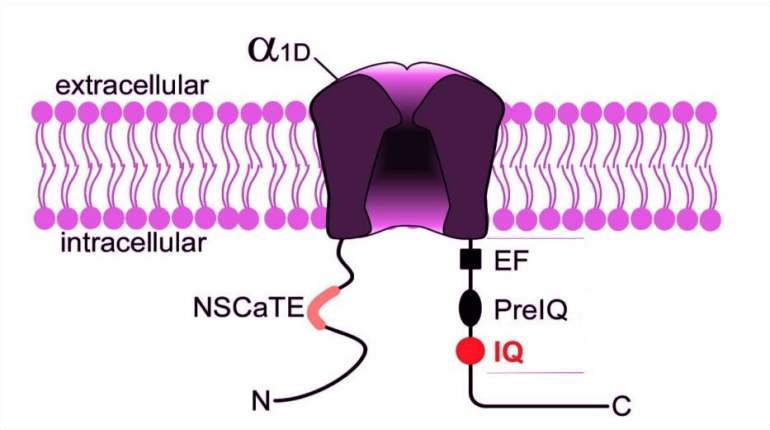

Figure 1. Schematic graph of the pore forming α1D subunit of $Ca_V1.3$ channel. NSCaTE at N-terminal (pink), EF hands, PreIQ domain (black) and IQ domain (red) at C-terminal are labeled.

Correspondingly, the elimination of $Ca_V1.3$ led to the complete absence of Ca^{2+} currents in the inner hair cells, which led to congenital deafness. Spike frequency adaptation was also reduced in the absence of $Ca_V1.3$ channels in mouse chromaffin cells (Vandael et al. 2012). The effect of deleting $Ca_V1.3$ channels in SAN was bradycardia (Mangoni et al. 2003, Platzer et al. 2000). Besides, inducible atrial flutter and fibrillation were observed in the $Ca_V1.3$-null mutant mice, and atrial arrhythmia in atrial myocytes was also observed with a depolarizing shift in the voltage-dependent activation of $\boldsymbol{I}_{Ca}$ (Platzer et al. 2000, Zhang et al. 2005c). Moreover, evidence obtained from $Ca_V1.3$-null mutant mice suggested the important role of $Ca_V1.3$ channel in the generation of β cell in postnatal pancreas (Namkung et al. 2001).

Further studies using $\alpha1D^{-/-}$ mice reported more phenotypic changes related to fear conditioning and mood disorders. It was reported that the consolidation of contextually conditioned fear was affected in the $\alpha1D^{-/-}$ mice. The $\alpha1D^{-/-}$ mice showed impaired LTP in amygdala and enhanced neuronal excitability in field recording from the basolateral complex of the amygdala (McKinney et al. 2009). One more recent study by the same group also reported that the $\alpha1D^{-/-}$ mice had reduced depression-like behavior as they had less time of immobility in forced swim and tail suspension tests (McKinney et al. 2009). These studies strongly supported the claim that $Ca_V1.3$ channels are important for fear memory and may play a role in amygdala related

brain functions and mood disorders like anxiety and depression.

In line with the findings in $Ca_V1.3$-null mice, a mutation in human CACNAD gene that codes for $Ca_V1.3$ was found in two consanguineous Pakistani families. The study indicated that the 1208_1209insGGG mutation would cause loss of function of the channels (Baig et al. 2011). The $Ca_V1.3$ channels that carried this mutation were non-conductive and as expected, subjects with homozygous mutations suffered from congenital deafness and SAN dysfunction (Baig et al. 2011). However, other clinical features in human due to loss of $Ca_V1.3$ current have not been chanracterized.

1.2.2 Role of $Ca_V1.3$ channels in suprachiasmatic nucleus regulating circadian rhythm

$Ca_V1.3$ channels may also play a role in regulating circadian rhythm. A group of neurons known as pacemakers in the suprachiasmatic nucleus (SCN) serves as part of the master control of the circadian rhythmic behaviors. The firing frequency of their spontaneous action potential changes rhythmically with light-dark cycles. It is known that the firing frequency is about 3-8 Hz during the day and mostly silent during the night (Pennartz et al. 2002, Colwell 2011). Several studies have shown that LTCCs contribute to Ca^{2+} influx that triggers spontaneous AP firing of the SCN neurons (Pennartz et al. 2002, Belle et al. 2009).

As the large conductance Ca^{2+}-activated potassium channels (BK channels) are one of the most important channels that regulate the firing frequency of neurons in SCN, the co-localization of $Ca_V1.3$ channels and BK channels may suggest coupling of these two channels (Vandael et al. 2010). It has been reported that the expression level and currents of BK channels are both circadian rhythmically regulated: the protein level was lower in the day than the night and the current is also smaller in the day than the night (Gilbert R. Pitts, Hidenobu Ohta and McMahon 2006). Meanwhile, Ca^{2+} currents were also shown to be diurnally modulated: larger in the day than the night and regular Ca^{2+} spikes could be observed during the day while it is absent during the night, which corresponds with the diurnally regulated firing frequency of SCN neurons (Pennartz et al. 2002).

By using the $\alpha1D^{-/-}$ mice, Vandael *et al* (2010) also found that deletion of $Ca_V1.3$ channels abolished the fast inactivation of BK channels while the slow inactivation was unaffected. This is a strong piece of evidence suggesting that $Ca_V1.3$ channels regulates the fast inactivation of BK channels by closely coupling with BK channels. However, compared to the weakened circadian amplitudes in multiple behaviors (for example, running wheel and home cage activity) and completely disrupted circadian rhythm observed in BK-null mice (Meredith et al. 2006), the $\alpha1D^{-/-}$ mice only showed moderate changes in circadian rhythm related behaviors, such as diminished activity during the night (Kent and Meredith 2008). It is thus clear that $Ca_V1.3$

channel is involved in circadian rhythmic regulation of pace-making activity of the SCN neurons. However, the underlying mechanism of how $Ca_V1.3$ channel contribute to the diurnal changes of spontaneous firing frequency is still largely unknown. Further study is needed to fill the gaps that remained.

1.2.3 Role of $Ca_V1.3$ channels in dopaminergic neurons in substantia nigra pars compacta nucleus (SNc)

Besides SCN, $Ca_V1.3$ channels had been shown to be important in the pace-making activity of neurons in the substantia nigra pars compacta nucleus (Chan et al. 2007). James Surmeier and his group have published several articles in recent years suggesting that $Ca_V1.3$ channel might be a potential therapeutic target to manage Parkinson's disease. In their studies, they found that there was increasing dependence on $Ca_V1.3$ for the influx of Ca^{2+} in the pace-making neurons in SNc during aging. Blocking of $Ca_V1.3$ channels could result in a reversion to juvenile form of pace-making activity (Chan et al. 2007).

The proposed hypothesis was that the increased influx of Ca^{2+} might lead to ER and mitochondria stress and their deleterious effects could accumulate over time during aging. This accumulating effect due to oxidative stress was claimed to be one of the causes that result in neuronal death. Oxidative stress seemed to be caused by the increasing energy consumed in buffering cytosolic Ca^{2+}. The

expression of Ca^{2+} buffering protein calbindin in ventral tegmental area (VTA) neurons helps to buffer the cytosolic Ca^{2+}. However, most dopaminergic neurons in SNc were found to be calbindin-negative (Cb^{-}). Neurons lacking of calbindin would therefore consume more energy to buffer cytosolic Ca^{2+}. Therefore, Cb^{-} neurons would be subject to enhanced oxidative stress and become more vulnerable to mitochondrial toxin (Mosharov et al. 2009, Surmeier et al. 2011a). These findings pointed to a new direction in understanding the pathology of Parkinson's disease.

One more recent study reported that Ca^{2+} entry during pace-making activity generated basal mitochondrial oxidant stress, which could worsen in a DJ-$1^{-/-}$ background. Mutations in DJ-1 have been associated with early-onset Parkinson's disease in human (Goldberg et al. 2012). Although there are growing evidences supporting the important role of $Ca_V1.3$ in oxidant stress, how $Ca_V1.3$ channels modulate SNc pace-making activity and how the function of these channels are regulated in these dopaminergic neurons during aging are not clearly understood. Knowledge of the underlying mechanism by which $Ca_V1.3$ channels are involved in pace-making activity and are contributing to the accumulation of oxidative stress would benefit research into the discovery of clinical therapy for Parkinson's disease.

1.3 Functional diversity of $Ca_V1.3$ channels generated by alternative splicing and RNA editing

The two kinds of post-transcriptional modifications, alternative splicing and RNA editing, are important mechanism that introducing diversity on the RNA level and leading to functional alterations of the translated proteins. $Ca_V1.3$ channel undergoes both alternative splicing and A-to-I RNA editing resulting in different isoforms that exhibit various electrophysiological and pharmacological properties.

1.3.1 Alternative splicing diversify $Ca_V1.3$ channel function

Alternative splicing is a process that particular exons of a gene from the pre-mRNA are included in or excluded on the mRNA. The $Ca_V1.3$ channel undergoes extensive alternative splicing at N-terminal, I-IV domains and C-terminal. Splicing variations in the C terminus strongly affect voltage-dependent activation, calcium-dependent inactivation, current density and drug sensitivities (Huang, Yu and Soong 2013, Huang et al. 2014).

1.3.2 A-to-I RNA editing

A-to-I RNA editing is one type of posttranscriptional modification that results in the recoding of genomic information. This mechanism contributes to the diversity of proteins and their functions. A-to-I RNA editing is catalyzed by a family of enzymes known as Adenosine Deaminase Acting on RNA (ADARs) that specifically bind to double-stranded RNA structure. This family has three mammalian members:

ADAR1, ADAR2 and ADAR3. During RNA editing, single adenosine is deaminated to inosine that is recognized as guanosine in mRNA translation resulting in recoding of a codon within the primary RNA transcript, and this leads to alteration in the expression and/or functional property of the target protein (Ashani and Bass 2012).

1.3.2.1 ADAR2 mediated RNA editing

Ion channels and neurotransmitter receptors are the major targets of ADAR2 mediated A-to-I RNA editing in the mammalian nervous system. RNA editing in the channels or receptors alters their gating properties or their ability to bind other interacting proteins.

The level of RNA editing at the Q/R site of GluA2 subunit of AMPA receptors (GluRs) is approximately 99%. AMPA receptors with edited GluA2 subunit is Ca^{2+} impermeable and editing will therefore modulate synaptic plasticity (Wright and Vissel 2012). AMPA receptors containing GluA2 with RNA editing at the R/G site showed enhanced rate of recovery from desensitization (Miyoko et al. 1993). Pharmacologically, RNA editing at the Q/R site resulted in reduced sensitivity of AMPA receptors to spider toxin (JSTX) (Streit and Decher 2011).

Similarly RNA editing at the I/V site of $K_V1.1$ channel affected the interaction of β subunits with different inactivation particles and reduced the binding affinity of channel blockers, which lead to enhanced the recovery from inactivation (Streit and Decher 2011,

Bhalla et al. 2004). The IC_{50} value of Psora-4 and 4-AP increased drastically to almost 70-fold when comparing to unedited channels, while the inhibition of arachidonic acid on $K_V1.1$ channel showed a negative correlation with editing level (Decher et al. 2010).

While editing of serotonin 2C receptors occurred at five closely located sites, the fully edited receptor exhibited the inactive conformation that had reduced coupling of receptors with G-protein and lower agonist affinity (Seeburg, Higuchi and Sprengel 1998, Busquet et al. 2010). RNA editing of 5-HT_{2C} receptors could also alter the agonist-directed trafficking of receptor stimulus (ADTRS), which means that because the edited receptor preferred to form the inactive conformation, the conformation promoted by receptor agonist that specifically couple to or activate certain downstream signaling cascades might be altered. Thus the edited receptor lost the ability to be directed by agonists to preferentially activate the PLC-PI or PLA2-AA pathways (Berg and Bush 2001). As different editing status resulted in activation of different downstream pathways, thus the effect of drug, beside the binding affinity, also strongly depended on the status of RNA editing. A recent study reported that higher level of edited 5-HT_{2C} were found in human suicide victims with high association of gene expression and DNA methylation (Di Narzo et al. 2014).

Another RNA editing substrate is $GABA_A$-α3 receptor. Researchers reported that I/M site editing of $GABA_A$-α3 receptor resulted in both

reduction of current and alteration of gating kinetics (Ohlson et al. 2007, Rula et al. 2008). The reduced currents might be caused by the impaired trafficking of $GABA_A$-α3 edited receptors to the surface. The editing level of I/M site of the $GABA_A$-α3 receptor has shown to be developmentally regulated. The editing level in mouse brain was about 5% at E15, rising up to over 90% at P21. With this increased level of RNA editing, the protein level of $GABA_A$-α3 receptor decreased after birth (Daniel et al. 2011).

These altered channel functions and receptor properties had also shown to be implicated in neurological diseases, such as in epileptic seizures, amyotrophic lateral sclerosis (ALS), and mood disorders like schizophrenia, depression and anxiety. Reduced RNA editing at Q/R site in GluA2 was detected in the motor neurons from ALS patients, which contributed to increased Ca^{2+} permeability of AMPA receptors (Yukio et al. 2004). Elevated editing level at the I/V site of K_V1.1 channels has been reported in chronic epileptic rat model, which showed reduced 4-AP sensitivity (Streit et al. 2011). Increased editing level at sites A, E and C in 5-HT_{2C} receptor was observed in patients suffering from schizophrenia or major depression, while the editing level at sites B and D seemed to be decreased (Gurevich et al. 2002).

For regulation of RNA editing, beside the duplex hairpin structure, a cis-acting element 150 nt downstream of the editing site of $GABA_A$-α3 receptor was recently reported to be able to induce site-specific editing

(Daniel et al. 2012). It strongly supported the idea that there could be cis-acting elements responsible for the regulation of RNA editing.

1.3.2.2 RNA editing in IQ domain of $Ca_V1.3$ channel

In the study by Huang et al (2012), it was reported that there are 3 sites within the IQ-domain of $Ca_V1.3$ that undergo A-to-I RNA editing. These result in recoding of amino acids: I/M, Q/R and Y/C. The IQ-domain is the site where calmodulin binds to trigger Ca^{2+}-dependent inactivation of $Ca_V1.3$, a negative feedback mechanism to close the channels. RNA editing was not detected in other regions of the α1D transcript. Furthermore, the IQ-domains of other Ca_V channels ($Ca_V1.2$, $Ca_V1.4$, $Ca_V2.1$, $Ca_V2.2$ and $Ca_V2.3$) were unedited.

Functionally, the edited forms, MQDY, IRDY and MRDY, of $Ca_V1.3$ IQ-domain showed different extent of attenuation of Ca^{2+}-dependent inactivation (CDI), as compared to the unedited $Ca_V1.3$ channels. However, editing at Y/C site did not show similar effects on the channel as the other two sites. No significant alterations of channel properties were detected. Interestingly, unlike I/M and Q/R editing that were conserved between rodents and human, the Y/C site was only edited in rodents but not in human.

Physiologically, RNA editing in $Ca_V1.3$ channel IQ domain is developmentally regulated. The occurrence of RNA editing is postnatal. The editing level increases during the first week after birth and almost

reaches the adult level at postnatal day 7 (Huang et al. 2012b). More interestingly, in this study, we also found that RNA editing in IQ-domain of $Ca_V1.3$ only occurred in the central nervous system (CNS). By using ADAR2$^{-/-}$/GluR-B$^{R/R}$ mice as a model, it was shown that elimination of RNA editing would result in lower firing frequency of pace-making activity in SCN suggesting the role of RNA editing in affecting pace-making activity.

1.4 Gaps and purposes

As discussed above, taking both the physiological roles of $Ca_V1.3$ channels and the CNS specificity of RNA editing in $Ca_V1.3$ IQ domain into consideration, it will be interesting to investigate the importance of $Ca_V1.3$ RNA editing in neurophysiology and in disease.

First, the contribution of LTCCs to the Ca^{2+} influx that drives the spontaneous pace-making activity was shown to be essential for the firing of pace-making neurons in both SCN and SNc (Jackson, Yao and Bean 2004). It was also reported that the elimination of RNA editing would result in lower firing frequency in SCN neurons (Huang et al. 2012b). As the SCN is the core region for central timing control, and the firing frequency is circadian rhythmically regulated, the roles and regulation of IQ-domain RNA editing of $Ca_V1.3$ in affecting the firing frequency of SCN neurons became an important question. To answer this question, the level of RNA editing will be evaluated at different time

points across 24 hours to establish the pattern of rhythmic regulation of the IQ-domain RNA editing in $Ca_V1.3$.

Second, there are growing evidences emphasizing the importance of $Ca_V1.3$ channels in pace making in SNc neurons. Deletion of $Ca_V1.3$ channels led to compensatory current conducted by HCN channels, similar to the juvenile state. This “rejuvenation” of dopaminergic neurons was shown to be protective (Chan et al. 2007). Therefore, researchers suggested that $Ca_V1.3$ could be a potential target for clinical therapy to manage patients with Parkinson’s disease (Chan, Gertler and Surmeier 2010). However, the underlying mechanism of what regulates Ca^{2+} influx via $Ca_V1.3$ channels and contributes to the growing dependence on $Ca_V1.3$ channels during aging is still largely unknown. One possible mechanism could be that RNA editing might play a role in regulating the Ca^{2+} influx through $Ca_V1.3$ channels. To test this hypothesis, the first step is to check whether the level of RNA editing in the IQ domain of $Ca_V1.3$ changes during aging. If it does, instead of blocking the whole channel, modulating the editing level may be an alternative approach for treatment.

Third, $Ca_V1.3$ channels were shown to be important for the consolidation of contextual fear conditioning, which is mainly associated with the activity of neurons in the amygdala (McKinney and Murphy 2006, McKinney et al. 2009). Moreover, the depression-like behavior observed in $\alpha1D^{-/-}$ mice further indicated the potential role of

$Ca_V1.3$ in mood disorders (Busquet et al. 2009). A question remains as to whether the level of RNA editing in the IQ domain of $Ca_V1.3$ is changed under mood disorders. Mood disorder mouse models will be used to evaluate the RNA editing level in different brain regions.

Overall, to fill the gaps in knowledge discussed above, the hypothesis is that (1) IQ-domain RNA editing in $Ca_V1.3$ is regulated under various physiological and pathological conditions. (2) Elimination of editing in $Ca_V1.3$ $ECS^{-/-}$ mice will influence the circadian rhythm, motoric function by affecting the pace-making activity of neurons in substantial nigra pars compacta (SNc) and suprachiasmatic nucleus (SCN). (3) Deletion of IQ-domain RNA editing may alter the mood disorder related behavior in $Ca_V1.3$ $ECS^{-/-}$ mice.

To address this hypothesis, this study investigates the potential roles of IQ-domain RNA editing of $Ca_V1.3$ channels and how they are modulated under different physiological and disease conditions, such as aging, circadian rhythm and mood disorders. For the purpose of this study, $Ca_V1.3$ $ECS^{-/-}$ mice were generated as a model in which RNA editing of IQ domain was specifically deleted. Studies using the $Ca_V1.3$ $ECS^{-/-}$ mice will provide further insights into the physiological significance of IQ-domain RNA editing of $Ca_V1.3$, and what behavioral outcomes may be affected.

1.5 Brief description of findings

Antisense oligonucleotide targeting the computationally predicted editing site complementary sequence (ECS) knocked down the editing level of α1D-minigene heterologously expressed in HEK 293 cells. This confirms the importance of the identified ECS in RNA editing of $Ca_V1.3$ IQ domain.

Based on this, $Ca_V1.3$ $ECS^{-/-}$ mice were generated using the global knockout strategy. In the $Ca_V1.3$ $ECS^{-/-}$ mice, RNA editing in the IQ domain was totally abolished. Characterization of the $Ca_V1.3$ $ECS^{-/-}$ mice showed that at the molecular level, the transcription and protein expression of Cacna1d was similar to the expression in WT mice. The C-terminal alternative splicing pattern was also unaffected. While behavioral characterization revealed (1) the $Ca_V1.3$ $ECS^{-/-}$ mice seemed to be more anxious than $Ca_V1.3$ WT littermate mice; (2) the $Ca_V1.3$ $ECS^{-/-}$ mice showed higher activity during the day, which might indicate disrupted sleep and altered circadian rhythm and (3) the overall motoric functions $Ca_V1.3$ $ECS^{-/-}$ mice seemed to be as normal as the WT littermate mice; but they exhibited slight deficit in balance.

As for the regulation of RNA editing of the IQ-domain under various physiological and pathological conditions, in the SCN editing level was

regulated in a circadian rhythmic fashion, while in SNc editing level was up regulated during aging. In the TPH2KI depression mice, no difference in RNA editing was detected.

In conclusion, the results from this study suggested that RNA editing in $Ca_V1.3$ IQ domain played important roles in (1) pace making activity of the SCN neurons and circadian rhythm; (2) oxidative stress of DA neuron in SN during aging; (3) anxiety disorders.

Chapter 2

Materials and Methods

2.1 Animals

C57BL/6J mice were used in the experiments. For circadian rhythm experiments, 4 week-old male mice were kept in the animal room with lighting control. For experiments that tissues were harvested in the light-on period, mice were habituated in the room with normal lighting control (7am-7pm light on) for two weeks before they were euthanized. While for experiments that tissues were harvested in the dark period, mice were habituated in the room with reverse lighting control (7am-7pm light off) for two weeks before they were euthanized as approved by the institutional IACUC. For depression experiments, *R439H_* TPH2Knock-in mice and WT control mice were obtained from collaborator Dr. Zhang Xiaodong, from the Duke-NUS Graduate School of Medicine.

2.2 Brain dissection and total RNA extraction

Whole brains were extracted from mice and then dissected into different brain regions. For aging experiments, whole brains were extracted from mice at age of 1.5 months, 12 months, 16 months and 24 months. For circadian rhythm experiments, whole brains were extracted for preparation of brain slices containing SCN region (detailed description Chapter 3.4). The SCN were punched out from the slices by blunt end needles. Total RNA was extracted by TRIzol method (Invitrogen, Carlsbad, CA). First strand cDNA was then synthesized using Superscript II and oligo (dT)18 primers (Invitrogen, Carlsbad, CA). Negative control reactions were also performed without

reverse transcriptase for all RT-PCR experiments to exclude contamination caused by genomic DNA.

2.3 Evaluation of RNA editing level in IQ domain of $Ca_V1.3$ channels

The RNA editing levels in IQ domain of $Ca_V1.3$ channels were evaluated by sequencing the PCR products of the fragment containing editing sites in IQ domain. The fragment was amplified by a pair of primers:

Forward primer 5'- CTCCGAGCTGTGATCAAGAAAATCTGG -3'

Reverse primer 5'- GGTTTGGAGTCTTCTGGCTCGTCA -3'

An amplicon of 299 bp would be detected on an agarose gel after electropheoresis.

For the RNA extracted from SCN, nested PCR was performed to amplify the fragment of editing sites in the IQ domain. The first round PCR was done using a pair of primers:

Out forward primer 5'- CAAGACTGAAGGGAACCTGG -3'

Out reverse primer 5'- TTGACATGGTTTCCAAGCAG -3'

An amplicon of 500 bp was produced.

A touch-down PCR protocol was used that included a 5-cycle decrement from 58 °C to 53 °C. The 30 cycles main PCR with denaturation at 94 °C for 30 sec, annealing at 53 °C for 30 sec, extension at 72 °C for 30 sec, and the final extension at 72 °C for 10

min. PCR products were then separated on a 1% agarose gel after electrophoeresis, extracted and purified using the Qiagen gel extraction kit. The PCR product was sent for direct automated DNA sequencing (1st Base, Singapore).

The level of RNA editing was calculated by measuring the heights of the peaks of A/G on the electropherograms obtained from DNA sequencing:

The editing level (%)=height (G)/[height (A)+height (G)]*100%

2.4 Antisense oligonucleotide knockdown

Antisense oligonucleotides (ASOs) with complementary sequences to 3 regions, the ECS (ASO) and its upstream (ASOI) or downstream (ASOII) sequence that include each of the three editing sites were used for knockdown of editing of $Ca_V1.3$ mini-gene expressed in the HEK 293 transfection system.

ASO: 5'- CCCTAAAACAGAATTGCTTC -3'

ASOI: 5'- AGAATTGCTTCAGAATATTC -3'

ASOII 5'- ATTCCATGCCACCACCCTAA -3'

HEK 293 cells cultured in DMEM with 10% (V/V) FBS were co-transfected with different amount of ASO (10nM, 25nM, 50nM and

100nM), 0.5 µg pRK5-gIQECS and 0.5 µg pIRES2-AcGFP1-ADAR2 by using Lippofectamine 2000 (Invitrogen) in 6-well plates.

The transfected HEK 293 cells were harvested 48 h after transfection and total RNA were extracted by using TRIzol method. The total RNA was first treated with RNase-free DNase (Ambion) and then subjected to reverse transcription using the reverse primer:

5'- GCGGTACCAATAAACAAGTTGGGCCATGG-3'.

PCR was performed to amplify the fragment containing editing sites with these pair of primers:

Forward primer: 5'-GGTGGCGCTTCCTATCGTTA-3'

Reverse primer: 5'-AGGGGCAGTGGGCAGTATCTC-3'

An amplicon of 560 bp was produced.

The level of RNA editing was evaluated by performing DNA sequencing of the PCR products using the forward primer.

2.5 Electrophysiological characterization of Y/C editing site

2.5.1 Construction of long-form and short-form $Ca_V1.3_{\alpha 1D}$ with edited/mutated IQ domain

In-vitro site-directed mutagenesis was performed with the following primers to substitute Y to E in the IQ domain of $Ca_V1.3$ channels to mimic phosphorylation at this site.

The $Ca_V1.3_{α1D\text{-}SF}$ and $Ca_V1.3_{α1D\text{-}LF}$ edited and mutated constructs named as $Ca_V1.3_{α1D\text{-}SF}$ IQDC, $Ca_V1.3_{α1D\text{-}LF}$ IQDC, $Ca_V1.3_{α1D\text{-}SF}$ IQDE and $Ca_V1.3_{α1D\text{-}LF}$ IQDE were generated from corrected $Ca_V1.3_{α1D}$ constructs (Hua Huang et al., 2013) by replacing a fragment of sequence containing the edited or mutated site into the corrected $Ca_V1.3_{α1D}$ construct. The fragment of sequence was first cloned into pGEMT-Easy vector, and then *in-vitro* site-directed mutagenesis was performed with the following pairs of primers to generate mutant $Ca_V1.3_{α1D\text{-}SF/LF}$ IQDE channels:

Forward primer: 5'- TCCTGATACAGGAC**GAG**TTTAGGAAATTCAA

Reverse primer: 5'- TTGAATTTCCTAAA**CTC**GTCCTGTATCAGGA

The protocol in the QuikChange Site-Directed Mutagenesis Kit was used (Stratagene, US) as according to the manual's instructions. The PCR program was 1 cycle 95 °C for 30 sec and followed by 16 cycles of 95 °C for 30 sec, 55 °C for 1min and 68 °C for 4min. The PCR product was digested with *DpnI* to remove the template plasmid before transformation.

The $Ca_V1.3_{α1D\text{-}SF}$ edited/ mutated clones were generated by replacing a fragment of sequence digested by *BstEII/NotI* containing the edited sites from uncorrected $Ca_V1.3_{α1D\text{-}SF}$ or pGEMT-IQ vector respectively into the corrected $Ca_V1.3_{α1D\text{-}SF}$ construct, while the edited/mutated $Ca_V1.3_{α1D\text{-}LF}$ subunit was generated by replacing a

fragment of sequence digested by *BstEII/KpnI* from $Ca_V1.3_{\alpha 1D\text{-}LF}$ or pGEMT-IQ vector respectively into the corrected $Ca_V1.3_{\alpha 1D\text{-}LF}$ construct.

2.5.2 Patch-clamp electrophysiology

All six kinds of channels SF-IQDY, SF-IQDC, SF-IQDE, LF- IQDY, LF-IQDC and LF-IQDE (1μg) were separately co-transfected with β_{2a} (1.25μg) and $\alpha_2\delta$ (1.25μg) subunits into HEK 293 cells. The HEK 293 cells were cultured with DMEM medium supplemented with 10% (v/v) Fetal Bovine Serum (FBS). About 48-72 hours after transfection, whole cell patch-clamp electrophysiology was performed to record the current under both Ba^{2+} and Ca^{2+}. The external solution contained 10 mM HEPES, 140 mM tetraethylammonium-methanesulfonate $(CH_3CH_2CH_2CH_2)_4N(CF_3SO_3)$, 5 mM $BaCl_2$ or $CaCl_2$ (pH 7.4 and osmolarity 290-310 mosM). The internal solution contained 130 mM Cs-$MeSO_3$, 5 mM CsCl, 5 mM EGTA, 10 mM HEPES, 1 mM $MgCl_2$, 2 mg/ml Mg-ATP (pH 7.3 and osmolarity 290 and 300 mosM).

Whole cell current filtered at 1-5 kHz and sampled at 5-50 kHz was obtained under voltage clamp with a Multiclamp 700 amplifier equipped with pCLAMP9.2 software (Molecular Devices, USA). Pipettes resistance was about 1.5-2 MΩ. The series resistance was less than 5 MΩ, before compensation by 80%. Currents were recorded with Ba^{2+} or Ca^{2+} as charge carrier by holding the cell at -90 mV, before stepping to various potentials from -60 mV to 50 mV for 1 s. In each cell, peak

currents at all voltages were normalized to the largest current observed (usually at -10 or -20 mV).

2.5.3 Data Analysis

Microsoft Excel and GraphPad Prism IV software (San Diego, CA) were used for data analysis. The data were then displayed as mean values ± SEM. Statistical significance of differences between means was calculated with two-tail, unpaired Student's T-test (Table 3.1 significant at $p < 0.05$). Calcium dependent inactivation data (Figure 3.2 B, Figure 3.2 C) were fitted by eye.

2.6 Generation of $Ca_V1.3$ ECS$^{-/-}$ mice

2.6.1 Generation of $Ca_V1.3$ ECS targeting construct

The strategy to generate ECS targeting construct is summarized in Figure 2.1. Briefly, a 9.2 kb mouse genomic DNA spanning 5.1 kb upstream and 4.1 kb downstream of ECS were digested from mouse bacterial artificial chromosome (BAC) DNA (Invitrogen, US) and subcloned into pBluescript SK+ vector. The ECS sequence was then replaced with the selection marker cassette containing the Neo^R gene flanked by loxP and FRT sites obtained from the NEB4 vector. Long-form and short form targeting constructs were generated. The sequence of the 3.5 kb targeting backbone containing 400 bp upstream of ECS, Neo cassette and 900 bp downstream of ECS was confirmed by automated DNA sequencing before digesting with *BsaBI*

and *BstBI* and re-ligated back into the CaV1.3-pBluescript SK+ vector to generate the long-form targeting construct. While the short-form targeting construct was subsequently generated from the long-form targeting construct by digesting long form construct with *BstBI* and *PmeI*. The *BstBI* site was retained after the ends were blunted and subsequently ligated.

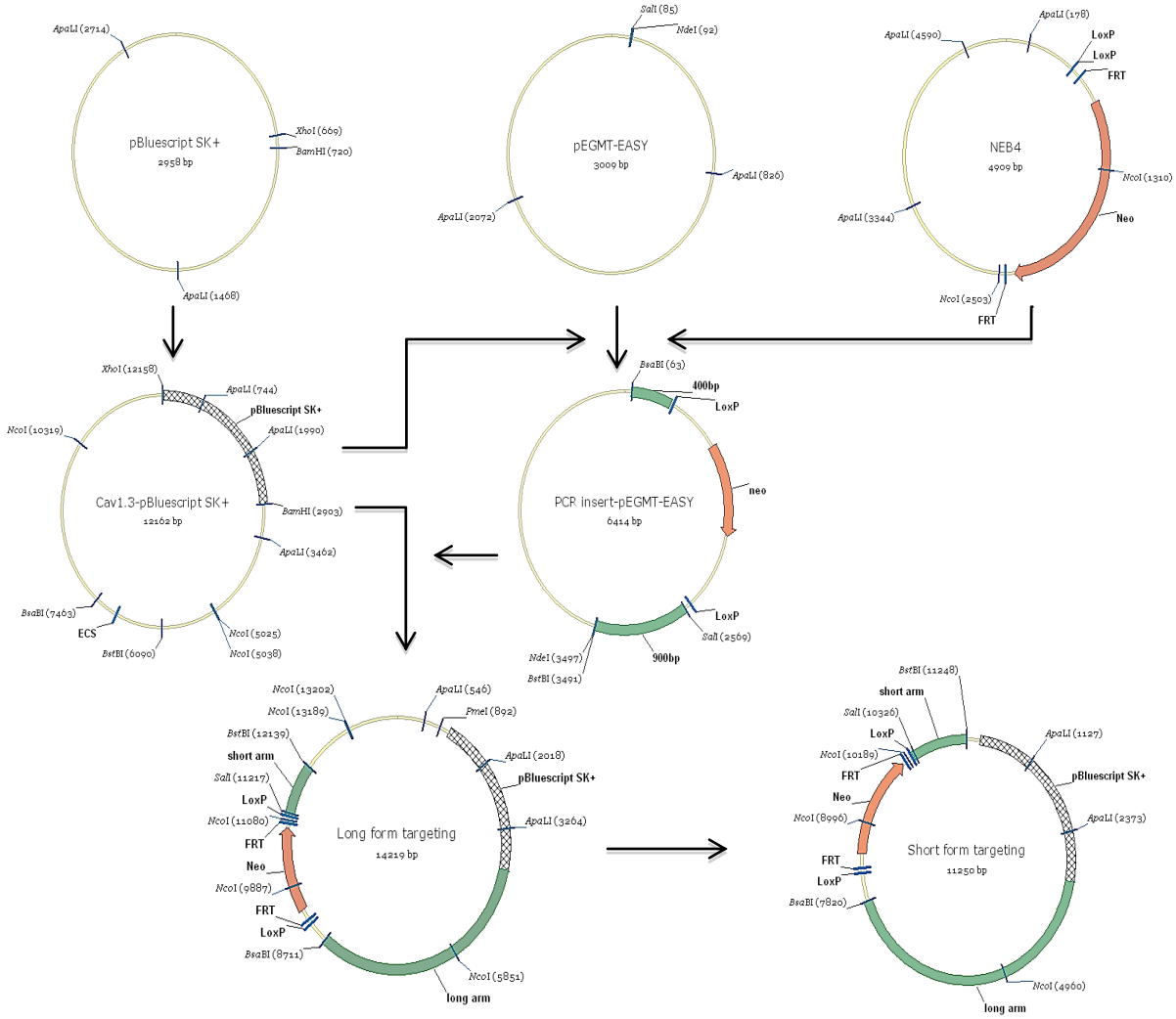

Figure 2.1. Flowchart showing the process for the generation of the short-form and long-form targeting constructs.

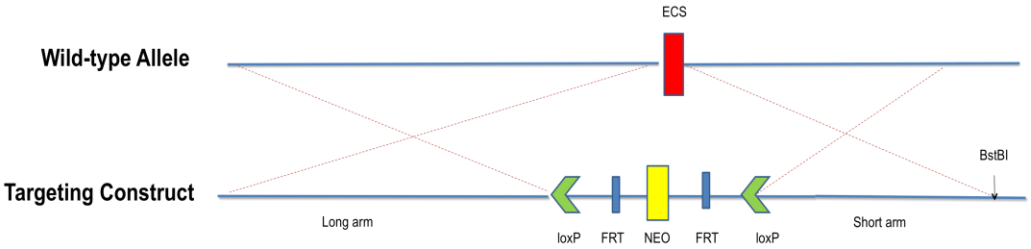

Figure 2.2. Schematic diagram of knockout strategy to delete ECS in m*Cacna1d* gene. The targeting construct was linearized using *BstBI* before transfecting into ES cells for homologous recombination.

2.6.2 Generation of ECS null mice

2.6.2.1 Culture of ES cells and identification of positive clones transfected with targeting construct

The MEF cells were cultured with MEF medium containing DMEM, 10% (v/v) FBS, 2mM glutamine, 100 units/mL Pen/Streps and 55 μM β-mercaptoethanol. After seeding of ES cells the medium changed to ES medium containing DMEM, 15% (v/v) FBS, 0.1 mM non-essential amino acids, 2 mM glutamine, 100 units/mL Pen/Streps, 55 μM β-mercaptoethanol and 1000 units/mL LIF.

The ES cells were first transfected with short-form targeting construct by electroporation (240 V 500 μF, 7.48 sec). Then after 250 μg/mL G418 neomycin drug selection, about 300 surviving colonies were picked into 96-well plates for further selection. The long-form targeting construct served as template for optimization of genotyping PCR and southern blot conditions for targeted ES colony selection. After optimization, the G418 resistant ES colonies were screened to

identify those that had undergone homologous recombination (Figure 3.7.2A and B).

The ES cell genomic DNA was extracted from 96-well plate by first adding lysis buffer containing 10 mM Tris-HCl (pH7.5), 10 mM EDTA, 10 mM NaCl, 10% (w/v) SDS and 1 mg/mL Proteinase K. And then the 96-well plates were incubated at 60°C O/N before adding 2×V of 100% cold ethanol to precipitate the genomic DNA. Centrifuging at 3000 rpm at RT for 20 min after incubation at RT for 30 min was performed to collect the precipitated DNA pellet. The DNA pellet was then washed by 70% ethanol and air-dried before elute with H_2O.

Genomic DNA extracted from ES cells was subjected to genotyping PCR to amplify a fragment from LoxP site to genomic sequence down stream of short arm with a pair of primers:

Fw1: 5'- ATGCTCCAGACTGCCTTGGGAAA -3'

Rs1: 5'- AGGCACAGCCTGCTATCCTGA -3'

An amplicon of 1.5kb in size indicated positive ES clones.

A touch-down PCR protocol was used that included a 5-cycle decrement from 58 °C to 53 °C. The 30 cycles main PCR with denaturation at 94 °C for 30 sec, annealing at 53 °C for 30 sec, extension at 72 °C for 90 sec, and final extension at 72 °C for 10 min. PCR products were then separated on a 1% agarose gel.

Southern blot was performed by first digesting the genomic DNA by restriction enzyme *NcoI*, and then the digested genomic DNA was ran on 0.7% agarose gel before transferred onto nitro membrane for hybridization with Probe I at 41 °C O/N. 5.3 kb band indicated WT allele while 2.1 kb band indicated recombined allele.

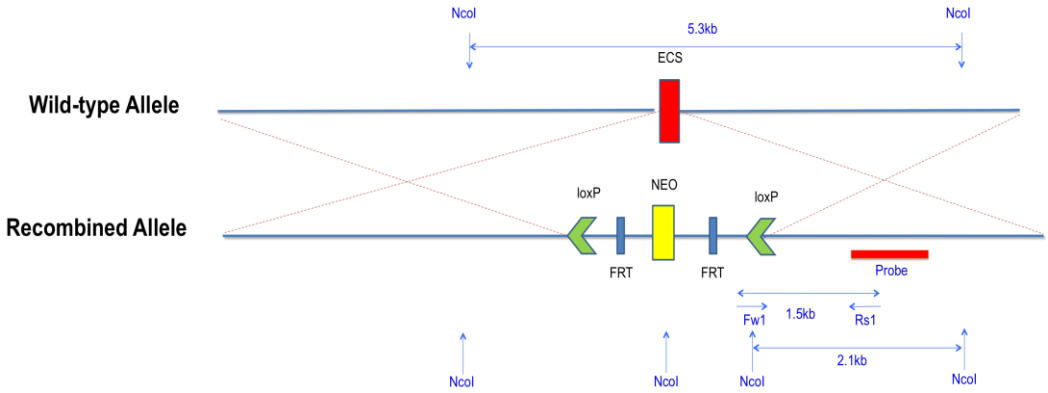

Figure 2.3. Genotyping strategy of identifying positive ES cells. Fw1 and Rs1 primers were used for genotyping PCR, NcoI digestion and probe was for southern blot analysis (in blue). ES cells undergo homologous recombination successfully showed 1.5 kb band in PCR, while 5.3 kb band indicating WT allele and 2.1 kb band indicating recombined allele in southern blot.

2.6.2.2 Microinjection of ES cells into SV129 mouse blastocysts

About 45 blastocysts were injected (Service from Biological Resource Centre Department I). Among the pups, 15 of them are chimeric mice. Male and high agouti-color coated F0 was selected to mate with C57BL/6 female mice to generate F1 pups.

2.6.2.3 Deletion of Neo cassette to generate $Ca_V1.3$ ECS$^{-/-}$ mice

To generate $Ca_V1.3$ ECS$^{-/-}$ mice, genotyping PCR and southern blot were performed to select male and female F1 with desired genotype Neo/WT for breeding to generate ECS null mice with Neo/Neo genotype (F2). F2 were then crossed with Actin-Cre mice for the deletion of selection maker Neo cassette (F3). To confirm the deletion, F3 mice were crossed with C57BL/6J to generate F4 with -/+ genotype. Then male and female F4 with desired genotype were crossed to generate $Ca_V1.3$ ECS$^{-/-}$ mice.

$Ca_V1.3$ ECS$^{-/-}$ mice were backcrossed with C57BL/6J mice for 6-10 generations to obtain >99% homology to C57BL/6J genetic background.

2.6.2.4 Genotyping strategy

Genotyping was performed with mice genomic DNA extracted from snipped tail. Tails were first digested with digestion buffer containing 10 mM Tris-HCl (pH7.5), 10 mM EDTA, 10 mM NaCl, 10% (w/v) SDS and 1 mg/mL Proteinase K at 55 °C O/N. The 1×V of phenol: chloroform: IAA (25:24:1) was added into digestion buffer, mixed well before centrifuging at 13,500 rpm at RT for 15 min. The supernatant was then transferred into new tube, followed by adding of isopropyl alcohol to precipitate DNA. Centrifuged at 3,750 rpm at 4 °C for 30 min after incubation at -20 °C for 1 hour to collect the DNA pellet. After washed with 70% ethanol air-dried pellet was eluted with 10mM Tris-HCl.

Then genomic DNA was used for genotyping by both PCR and southern blot. For the genotyping of F1 mice, the same strategy was used as for selection of positive ES cells.

For genotyping of F2 mice, triple primers PCR was performed (Fw1, Fw2 and Rs2, Figure 2.4 Black).

Fw1: 5'- ATGCTCCAGACTGCCTTGGGAAA -3'

Fw2: 5'- TGGTCGCATGGCTTAGATG -3'

Rs2: 5'- GGAGTGTTGCAGGCTCGTGA -3'

A 400 bp amplicon would indicate the allele with Neo cassette insertion, while a 256 bp amplicon identified the WT allele.

A touch-down PCR protocol was used that included a 5-cycle decrement from 65 °C to 60 °C. The 30 cycles main PCR with denaturation at 94 °C for 30 sec, annealing at 60 °C for 30 sec, extension at 72 °C for 30 sec, and the final extension at 72 °C for 10 min. PCR products were then separated on a 1% agarose gel.

The same restriction enzyme and probe were used in southern blot as described previously for genotyping of ES clones.

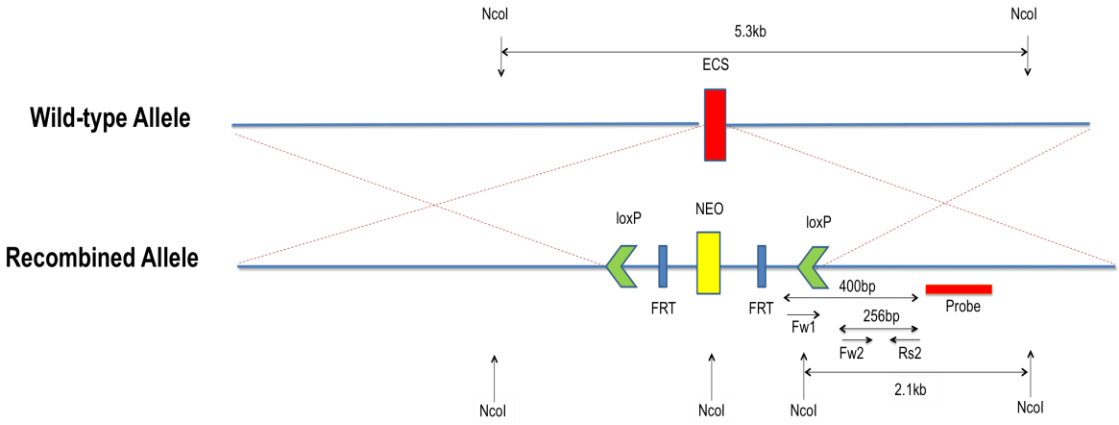

Figure 2.4. Genotyping strategy of identifying F1 agouti mice. Fw2 and Rs2 primers were used for genotyping PCR, *NcoI* digestion and probe was used for southern blot (in black). F1 mice with Neo/+ genotype showed 348 bp band in PCR, while both 5.3 kb and 2.1 kb bands in southern blot analysis.

For genotyping of F3 Cre-crossed and F4 mice, LoxP Fw and Rs2 primers were used in the PCR (Figure 2.5).

LoxP Fw: 5'- ATAACTTCGTATAATGTATGC -3'

Rs2: 5'- GGAGTGTTGCAGGCTCGTGA -3'

An amplicon of 191 bp would indicate the Neo-cassette deleted allele, while the WT allele would not be amplified.

A touch-down PCR protocol was used that included a 5-cycle decrement from 60 °C to 55 °C. The 30 cycles main PCR with denaturation at 94 °C for 30 sec, annealing at 55 °C for 30 sec, extension at 72 °C for 30 sec, and the final extension at 72 °C for 10 min. PCR products were then separated on a 1% agarose gel.

The same restriction enzyme and probe were used in southern blot as described previously.

For genotyping of $ECS^{-/-}$ mice and the following generations of backcrossed mice, two pairs of primers were used in two separate PCR reactions (Figure 2.5).

LoxP Fw: 5'- ATAACTTCGTATAATGTATGC -3'

Rs2: 5'- GGAGTGTTGCAGGCTCGTGA -3'

An amplicon of 191 bp would show up for the KO allele with same PCR program described previously.

ECS Fw: 5'- TGTTTTAGGGTGGTGGCATGGA -3'

Rs2: 5'- GGAGTGTTGCAGGCTCGTGA -3'

An amplicon of 145 bp would indicate the WT allele.

A touch-down PCR protocol was used that included a 5-cycle decrement from 65 °C to 60 °C. The 30 cycles main PCR with denaturation at 94 °C for 30 sec, annealing at 60 °C for 20 sec, extension at 72 °C for 20 sec, and the final extension at 72 °C for 10 min. PCR products were then separated on a 1% agarose gel.

For southern blot, the genomic DNA was digested by *SspI* restriction enzyme O/N before running on 0.7% agarose gel. Probe II was used at 41 °C for hybridization as described previously. 11 kb band indicated KO allele while 5.3 kb band indicated WT allele.

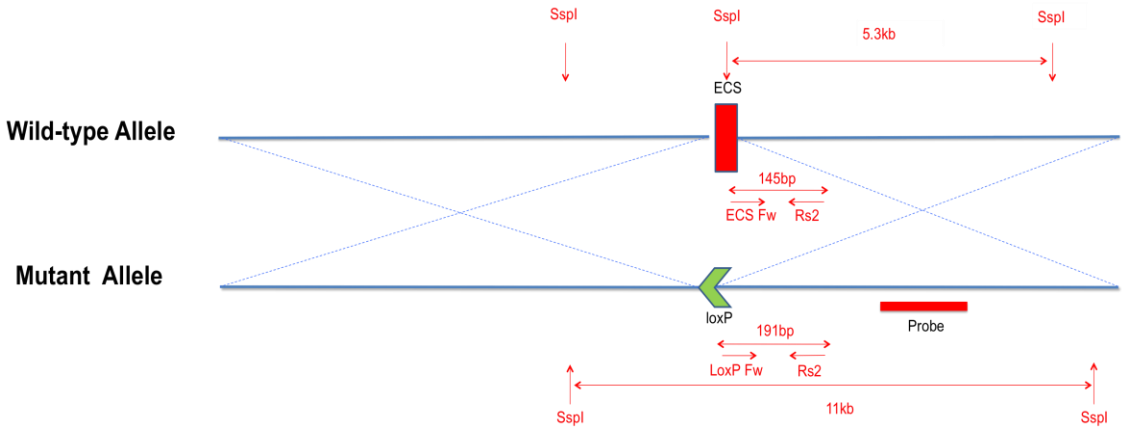

Figure 2.5. Genotyping strategy of identifying ECS knockout mice. ECS Fw, LoxP Fw and Rs2 for genotyping PCR, SspI digestion and Probe for southern blot analysis (in red). Homozygous mice (-/-) showed no band in PCR with ECS Fw and Rs2, 191 bp band in PCR with LoxP Fw and Rs2 and only 11 kb band in southern blot. Heterozygous mice (-/+) showed both 145 bp band in PCR with ECS Fw and Rs2 and 191 bp band in PCR with LoxP Fw and Rs2, while both 11 kb and 5.3 kb band in southern blot. Wild-type mice (+/+) showed 145 bp band in PCR with ECS Fw and Rs2, no band in PCR with LoxP Fw and Rs2 and only 5.3 kb band in southern blot.

2.7 Characterization of ECSKO mice

2.7.1 Evaluation of RNA editing level in IQ domain of $Ca_V1.3$ in whole brain

Total RNA was extracted by using TRIzol method (Invitrogen, Carlsbad, CA) from whole brain of both ECSKO mice and their WT littermates. First strand cDNA was then synthesized using Superscript II and oligo (dT18) primers (Invitrogen, Carlsbad, CA). Negative control

reactions were also performed without reverse transcriptase for all RT-PCR experiments to exclude contamination caused by genomic DNA. RNA editing level of both KO and WT mice were evaluated by the same method described in chapter 2.3. The same total RNA was also subjected to Real-time PCR and investigation of alternative splicing pattern.

2.7.2 Evaluation of transcription and protein expression level of Cacna1d in whole brain

The total RNA obtained as described previously was normalized to the concentration of 1 mg/μl after DNase treatment and then used for reverse transcription synthezing first strain DNA. The transcription level was detected using Taqman gene expression assay (Applied Biosystems, CA, USA). The transcription level of mCacna1d gene (Mm01209919_m1, NM_028981.2) was detected and normalized to the level of internal control gene Actb (Mm00607939_s1, NM_007393.3). The real-time PCR was run by 7500 real-time PCR system according to the manufacturer's instructions. ΔC_T value was used for statistic analysis by two-tails, unpaired Student's T-test.

Total protein was extracted from whole brain of both ECSKO and WT mice by first homogenizing the brain tissue in lysis buffer (150 mM NaCl, 30 mM HEPES, 10 mM NaF, 1% Triton X-100 and 0.01% SDS, pH 7.5) with freshly added cocktail proteinase and phosphatase inhibitors (Roche) and then rotated at 4 °C for 3 hours before

centrifuging at 13,500 rpm 4 °C for 15 min. Supernatant was collected and protein content was determined using Bradford assay (Pierce). Normalized amount of protein samples were mixed with loading buffer and incubated at 55 °C for 10 min. The samples were then resolved on 10% SDS-PAGE gel before transferring on nitrocellulose membrane (Thermo Scientific) and blocked with 5% non-fat milk in TBST (50 mM Tris-base, 150 mM NaCl, 0.1% Tween 20) before probing with antibodies and detecting using ECL reagent (Pierce). For detection of $Ca_V1.3$ channels, pAb_$Ca_V1.3_{42}$ antibody (Tan et al. 2011) was used at 1:200 for incubation overnight at 4 °C. Goat anti-rabbit secondary antibody was used at 1:2000 (Sigma) 1hour at room temperature. The level of β-actin in the input was detected as internal control. Anti-β-actin antibody was used at 1:10,000 (Sigma). And HRP-conjugated anti-mouse secondary antibody was used at 1:3000 (Sigma). The densities of bands on the blot were measured by using Image J. The relative expression level was calculated by normalizing to the level of β-actin. The expression levels were compared by two-tails, unpaired Student's T-test.

2.7.3 Investigation of C-terminal alternative splicing pattern of $Ca_V1.3$ channels

The first strand DNA obtained from both $Ca_V1.3$ $ECS^{-/-}$ and WT mice as described previously were used as template to amplify a fragment of the C-terminal of $Ca_V1.3$ channels containing Ex40-48 using the following pair of primers:

MusCTail Fw: 5’- AACCTCTTTGTGGCTGTCATC -3’

MusCTail Rs: 5’- GGGTCTGGCTCCTCGTCACT -3’

An amplicon of 2kb was produced.

The PCR products were then used as template for examination of splicing patterns within this fragment after they were separated on a 1% agarose gel extracted and purified using the Qiagen gel extraction kit.

The primers used for analyzing detailed splicing patterns in the C-terminal were listed in Table 2.1.

Table 2.1 Primer used to amplify across each splicing junction for the detection of exon combinations at the C-terminal of $Ca_V1.3$ channels.

40_F	5’- GAACCTGGAGCAAGCTAATGAAG -3’
41_R	5’-CTGTAGGGCAATCGTGGTGTT -3’
42_R	5’- CATCTTCTTCTTCTGGTTTGGAGT -3’
42_F	5’- AATCCGACGGGCTATATCCTGTGA -3’
43_R	5’- TCGATCATGCTTGCAGGAGTAA -3’
43_F	5’- CAGCATTGGGAACCTTGAG -3’
45_R	5’- CCAAGCAGCGGGGGTCTC -3’
47_F	5’- GCAAAGCAGCCAAGACGA -3’
48_R	5’- AGACTAGCTGGCGTGAAAG -3’

2.7.4 Characterization of electrophysiological properties of pace-making neurons

2.7.4.1 SCN slice preparation

Both $Ca_V1.3$ $ECS^{-/-}$ and $Ca_V1.3$ WT mice were maintained on a 12 hours light dark cycle using normal room light. The 200 µm coronal brain slices containing suprachiasmatic nucleus were obtained from P28-40 mice. All procedures were approved by the IACUC of the National University of Singapore. Mice were first anesthetized with isoflurane and then decapitated for preparation of brain slices on the vibrating blade microtome VT1000 S (Leica biosystems, US). The slicing chamber filled with oxygenated ice-cold cutting solution containing 125 mM NaCl, 2.5 mM KCl, 1.25 mM NaH_2PO_4, 25 mM $NaHCO_3$, 1 mM $MgCl_2.6H_2O$, 1 mM $CaCl_2$, 1 mM kynurenic acid, 0.005 mM glutathione, 0.1 mM N-nitro-I-argine, 0.5 mM ascorbic acid and 14 mM glucose (pH 7.5, 300-310 mosM). Slices were incubated at room temperature in incubation solution containing: 125 mM NaCl, 2.5 mM KCl, 1.25 mM NaH_2PO_4, 25 mM $NaHCO_3$, 1 mM $MgCl_2.6H_2O$, 2 mM $CaCl_2$, 1mM kynurenic acid, 0.005 mM glutathione, 0.1 mM N-nitro-I-argine, 14 mM glucose (pH 7.5, 300-310 mosM), bubbled with 95% O_2 and 5% CO_2 for 1-2 hours before recording.

2.7.4.2 Whole-cell recording in SCN slices

Current-clamp recording were conducted using EPC-9 amplifier controlled by Patchmaster (Heka Elektronik, Lambrecht, Germany).

Resistances of 4–6 MΩ pipettes were used. The internal solution contained: 140 mM $KMeSO_4$, 5 mM KCl, 0.05 mM EGTA, 10 mM N- (2-hydroxyethyl) piperazine-N'-ethanesulfonic acid (HEPES), 0.4 mM Na_3-GTP, 2 mM Mg-ATP and 10 mM Na-Phosphocreatine (pH 7.4, 290-300 mosM). Brain slices were transferred into the recording chamber of the upright fixed stage microscope equipped with 40X water immersion lens and constantly perfused with oxygenated ACSF (125 mM NaCl, 2.5 mM KCl, 1.25 mM NaH_2PO_4, 25 mM $NaHCO_3$, 1 mM $MgCl_2.6H_2O$, 2 mM $CaCl_2$, 14 mM glutamate, pH 7.5, 300-310 mosM) at a flow rate of 1.5 to 2 ml/min at room temperature. The SCN was identified as a bilaterally symmetrical, superior to the optic chiasm and lateral to the third ventricle (Pennartz et al. 1998). Individual SCN neurons were identified by IR-DIC camera. Cluster I SCN neurons in the dorsal medial shell were patched (Colwell 2011). The cluster I neurons were identified by their steeply rising and monophasic AHP (Pennartz et al. 1998). The membrane potential was corrected for the liquid junction potential -14.5 mV (Huang et al. 2012a). After formation of gigaseal (>3 GΩ), input resistance was monitored regularly by measuring voltage response by a -20 pA current injection. The spontaneous firing of action potential was recorded under current clamp.

2.7.5 Characterization of anxiety, motor function and circadian rhythm related behaviors

All the procedures are approved by IACUC of the National University of Singapore. The behavioral studies were performed within the

Neuroscience Phenotyping Core. Only male mouse was used in the tests.

2.7.5.1 Elevated Zero Maze

The elevated zero maze was used to test the anxiety level of both $Ca_V1.3$ $ECS^{-/-}$ and $Ca_V1.3$ WT mice. The mice were habituated in the behavior room at lease 1 hour before the test. During the test, they were allowed to freely explore a zero-shaped maze with open arms and closed arms. The maze is elevated at approximately 50 cm. The subjects are allowed to explore the maze for up to 8 min. The performance of each mouse was video recorded for data analysis. The number of transitions between the open and closed arms, the amount of time spend on the open arms were recorded and scored by using Ethnovision XT9. The average percentage of time spending on the arm, the number of transitions and the total distance traveled were compared between $Ca_V1.3$ $ECS^{-/-}$ and $Ca_V1.3$ WT mice using two-tail, unpaired Student's T-test (significant at $p<0.05$).

2.7.5.2 Rota-rod Test

The rota-rod test was conducted to assess the motor coordination and balance (Brooks and Dunnett 2009). Mice were habituated in the behavior room 30 min before the test. An accelerating protocol was used. Before starting the test, mice were placed on the rotor with the minimum speed at 4 rpm for 30 sec to inform the mice about the test and let them stabilize on the rotor as well. The rotor was speeded up to

maximum 40 rpm in 240 sec. The latency to fall in sec was recorded. The whole test lasted for 4 continuous days with 4 trials on each day for each mouse and 15 min rest in between trials. The average of 4 trials was taken for analysis. The latency to fall was compare on each day between $Ca_V1.3$ $ECS^{-/-}$ and $Ca_V1.3$ WT mice using two-tail, unpaired Student's T-test (significant at $p<0.05$). The learning curve was plotted with the average latency on each testing day by using GraphPad Prism IV software (San Diego, CA).

2.7.5.3 Balance Beam Test

The balance beam test assesses the ability of mouse to balance while crossing a narrow beam (Brooks and Dunnett 2009). Beams 50 mm in length, with two different widths, 6 and 12 mm, will be used in the balance beam test for training and testing. A bright light is used as an aversive stimulus at the start platform and an escape box (20x20x20 cm) is placed at the end of the beam. The mice were trained for three trials on the 12 mm beam and one trial on the 6 mm beam on the first day before the test trials and then the mice were given a two-day break before being tested on two consecutive days. The time taken to traverse the beam was recorded for each trial. The maximum time cutoff was 60s. On test-days 1 to 3, the number of slips and grips were also recorded. The time spent to cross the balance beam and the number of foot slips were compare on each day between $Ca_V1.3$ $ECS^{-/-}$ and $Ca_V1.3$ WT mice using two-tail, unpaired Student's T-test (significant at $p<0.05$). The learning curve was plotted with the average

time spend for crossing and number of foot slips on each testing day by using GraphPad Prism IV software (San Diego, CA).

2.7.5.4 Running Wheel Test

Running wheel (Wheel running) test is to measure the locomotor activity of mouse by the tendency of the mice to run on the wheel when one is provided in the home cage (Brooks and Dunnett 2009). Mice were housed singly with one running wheel provided for each of them together with food and water supply. The test was conducted over 48 hours under 12 hours light dark cycle. Before the start of test, mice were habituated in the cages for at lease 2 hours with the running wheel inside. The whole test was video recorded for data analysis. The mice were tracked by the camera and their activity and time spend on running wheel were scored by using Ethnovision XT9. The percentage of time spent on the running wheel during day and night were compared between $Ca_V1.3$ $ECS^{-/-}$ and $Ca_V1.3$ WT mice using two-way ANOVA (significant at $p<0.05$).

Chapter 3

Results

3.1 Experimental research strategy

To characterize functional RNA editing of $Ca_V1.3$ channel, the research strategy used in the thesis is summarized in Figure 3.1. First, in previous study, different from the other two editing sites, no functional effect was detected for Y/C editing. Therefore, to investigate the effect of Y/C editing on channel properties, mimicking of tyrosine phosphorylation was conducted to reveal the relationship between Y/C editing and tyrosine phosphorylation. Second, as IQ-domain RNA editing occurred widely in CNS, it would be interesting and important to know whether the editing level was modulated under various physiological and pathological conditions. Change of editing level in substantia nigra in aging, modulation of editing level in suprachiasmatic nucleus with circadian rhythm as well as editing level in amygdala and hippocampus were determined. Third, to better assess the physiological significance of IQ-domain RNA editing in $Ca_V1.3$ channels, $Ca_V1.3$ $ECS^{-/-}$ mice were generated based on deletion of the ECS identified by ASO knockdown. Further characterization of $Ca_V1.3$ $ECS^{-/-}$ mice were performed on molecular, electrophysiological and behavioral levels.

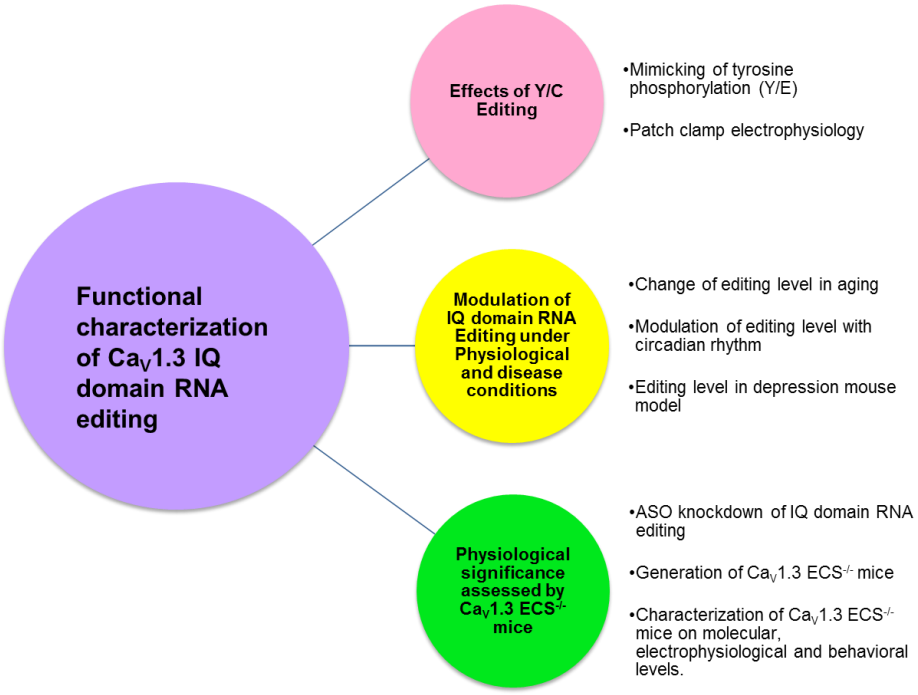

Figure 3.1 Schematic graph of research approaches in this thesis.

3.2 Functional effect of Y/C editing site is related to phosphorylation at this site in a splice variant dependent manner.

In previous study, unlike the other two editing sites (I/M and Q/R), the Y/C editing did not result in any functional change of channel properties. However, the level of editing at Y/C site was always detectable and had shown to be regulated under different physiological conditions. Therefore, it raises the question about what functional effect Y/C editing may have on $Ca_V1.3$ channels. One possibility is that Y/C editing could affect putative tyrosine phosphorylation. As predicted by a online programme in Kinexus|PhosphoNET (http://www.phosphonet.ca), the tyrosine in IQDY (Y_{1615}) is a potential tyrosine phosphorylation site (Figure 3.2 A). There are 50 human tyrosine kinases predicted, for example KDR, Flt4, MER and JAK2, that can potentially phosphorylate the tyrosine at IQDY (http://www.phosphonet.ca/kinasepredictor).

Previous studies from David Yue's group showed that tyrosine (Y_{1615}) to alanine substitution at the Y/C editing site resulted in neither change of CDI nor binding affinity of Ca^{2+}/CaM (Bazzazi et al. 2013). However, tyrosine (Y_{1615}) to aspartic acid substitution, mimicking tyrosine phosphorylation did not affect CDI but had reduced binding affinity to Ca^{2+}/CaM (Ben Johny et al. 2013). These evidences indicated that tyrosine phosphorylation at the Y/C editing site might affect the binding affinity of Ca^{2+}/CaM.

To test the effect of phosphorylation of Y_{1615} on channel, a mutant channel was generated with substitution of Y to E, which mimicked the structure of phosphorylation at the tyrosine site. As was shown in previous study, the $Ca_V1.3$_LF (Ex42) or $Ca_V1.3$_SF (Ex42a) channels have various strength of CDI (Huang et al. 2013). Whole cell path-clamp electrophysiology was performed with wild-type $Ca_V1.3$_IQDY channels, edited $Ca_V1.3$_IQDC channels and mutant $Ca_V1.3$_IQDE channels in the backbone of either the short-form (Ex42a) or long-form (Ex42) splice variant. CDI was compared among SF-IQDY, SF-IQDC and SF-IQDE as well as among LF-IQDY, LF-IQDC and LF-IQDE. As the remaining peak Ba^{2+} current after 50 ms depolarization to various potentials (r50) indicated voltage-dependent inactivation (VDI), pure CDI was quantified by the f-value, calculated as the difference in r50 measured in Ba^{2+} and Ca^{2+} at -10 mV.

For SF-$Ca_V1.3$ channels, the difference in r50 was insignificant between SF-IQDY (f=0.76±0.02) and SF-IQDC (f=0.73±0.01), while SF-IQDE showed clearly less CDI (f=0.59±0.02) at 50 ms (Figure 3.2 B, Table 3.1). For LF-$Ca_V1.3$ channels, both LF-IQDC (f=0.19±0.03) and LF-IQDE (f=0.17±0.03) showed slightly reduced CDI at 50 ms than LF-IQDY (f=0.26±0.01), although there was no significant difference between the two of them.

The results indicated that in the context of SF-$Ca_V1.3$, the mimicking of phosphorylation at Y_{1615} would lead to impaired CDI. The edited SF-IQDC displayed similar CDI as SF-IQDY, but has lost the ability to be phosphorylated and show attenuated CDI. While in the context of LF-$Ca_V1.3$, the mimicking of phosphorylation at Y_{1615} revealed similar CDI as LF-IQDC and LF-IQDY. It seemed that phosphorylation at Y_{1615} did not affect CDI of LF-$Ca_V1.3$ channels as it did on the SF-$Ca_V1.3$ channels. It raises new questions about why the effects of RNA editing or phosphorylation at Y_{1615} are different on SF-$Ca_V1.3$ and LF-$Ca_V1.3$ and how they may be regulated.

A

Site 142	Y1469	V	I	M	D	N	F	D	Y	L	T	R	D	W	S	I
Site 143	Y1492	F	K	R	I	W	S	E	Y	D	P	E	A	K	G	R
Site 144	Y1615	A	T	F	L	I	Q	D	Y	F	R	K	F	K	K	R
Site 145	Y1631	E	Q	G	L	V	G	K	Y	P	A	K	N	T	T	I
Site 146	Y1806	S	S	V	K	R	T	R	Y	Y	E	T	Y	I	R	S

B

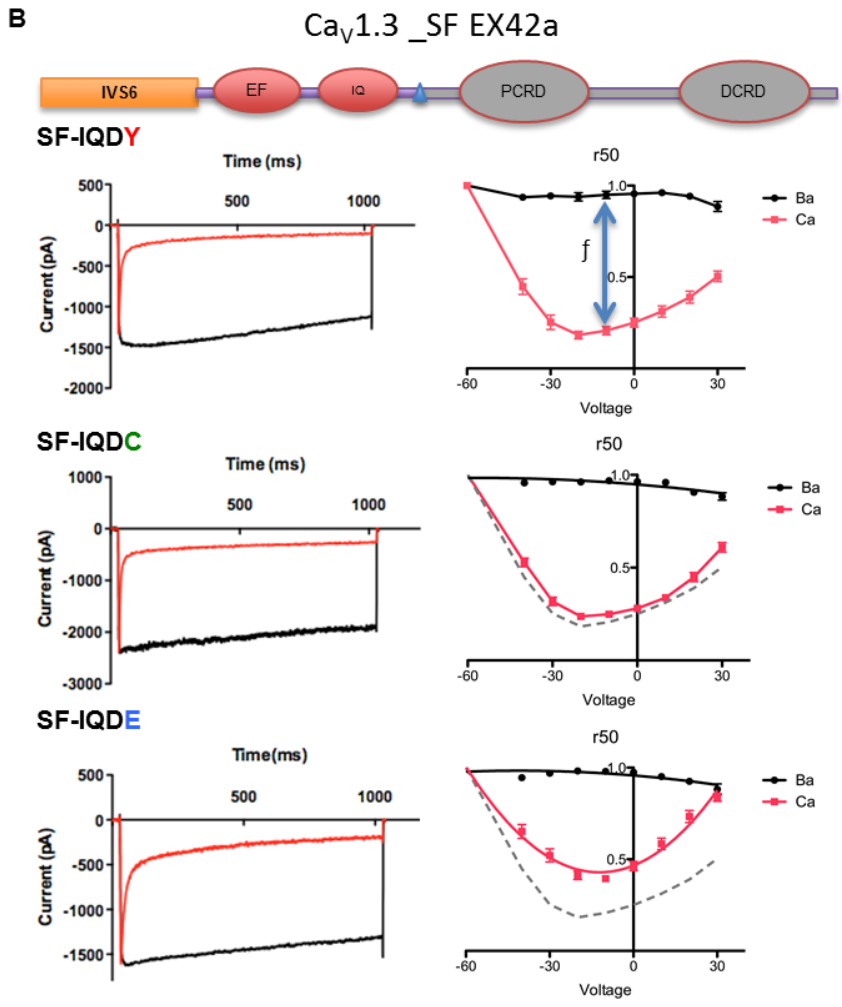

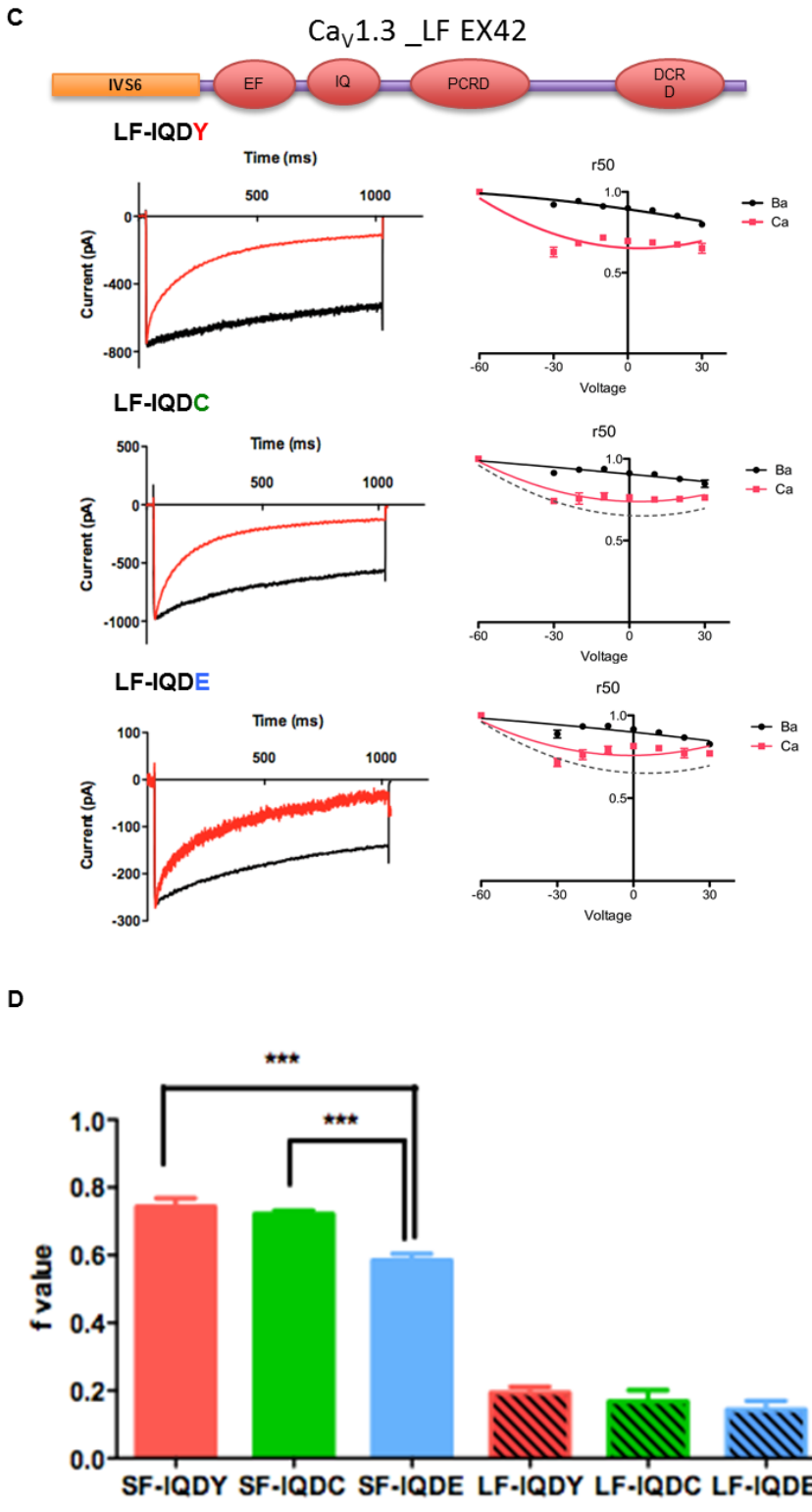

Figure 3.2 Modulation of IQ domain RNA editing by mimicking of phosphorylation at tyrosine site in both SF-Ca$_V$1.3 and LF-Ca$_V$1.3 channels. A. Prediction of phosphorylation site at Y1615 (red box). B. Comparison of CDI in the context of SF-Ca$_V$1.3 channels. Top panel, schematic diagram

demonstrating the structure context of SF-$Ca_V1.3$ channels. Bottom panel, left, exemplar trace of currents evoked from -90 mV holding potential to -10 mV test potential, with Ba^{2+} as charge carrier (black), Ca^{2+} as charge carrier (red). Throughout, vertical scale bar pertains to Ca2+ current, and Ba2+ currents are scaled down to facilitate visual assessment of kinetic decay. Right, averaged inactivation profiles of SF-IQDY (Upper), SF-IQDC (Middle), and SF-IQDE (Bottom) shown by r50, the fraction of peak currents remaining after 50-ms depolarization to indicated voltages (V), with Ba^{2+} as charge carrier (black), Ca^{2+} as charge carrier (red) C. Comparison of CDI in the context of SF-$Ca_V1.3$ channels. Top panel, schematic diagram demonstrating the structure context of LF-$Ca_V1.3$ channels. Bottom panel, left, exemplar trace of currents evoked from -90 mV holding potential to -10 mV test potential, with Ba^{2+} as charge carrier (black), Ca^{2+} as charge carrier (red). Right, averaged inactivation profiles of LF-IQDY (Upper), LF-IQDC (Middle), and LF-IQDE (Bottom) shown by r50. D. Average f-value of SF-IQDY, SF-IQDC, SF-IQDE, LF-IQDY, LF-IQDC, and LF-IQDE. (Statistics shown under Table 3.1)

Table 3.1 Ca^{2+}-dependent inactivation of $Ca_V1.3$ channels in comparison with different SF/LF and edited/mutant variants

Construct	f-value at r50
SF-IQDY (11)	0.76±0.02***
SF-IQDC (15)	0.73±0.01***
SF-IQDE (10)	0.59±0.02
LF-IQDY (8)	0.26±0.01
LF–IQDC (7)	0.19±0.03
LF–IQDE (10)	0.17±0.03

Number of experiments is indicated in parentheses. For statistics, *** p<0.001,

f-value at r50 of $Ca_V1.3$_IQDY or $Ca_V1.3$_IQDC compared with $Ca_V1.3$_IQDE (One-way ANOVA).

3.3 Increase in RNA editing of IQ domain in substantia nigra in aging

Increased expression level of $Ca_V1.3$ channels in cortical neurons of patients with early stage Parkinson's disease has been reported (Hurley et al. 2013). The growing dependence on $Ca_V1.3$ channels for the influx of Ca^{2+} into the dopaminergic neurons in SNc has also been shown to play an important role in mitochondrial and ER stress. This may partially contribute to cell death during aging or in the development of Parkinson's disease. However, how RNA editing of $Ca_V1.3$ IQ domain modulates influx of Ca^{2+} to affect pace making in SNc neurons and how it is regulated during aging are still unclear.

To address this question, the substantia nigra regions were obtained from male C57BL/6 mice at ages of 1.5-month (n=3), 12-month (n=6), 16-month (n=3) and 24-month (n=5) for evaluation of RNA editing levels. The results showed that the editing level of $Ca_V1.3$ was increased in SN during aging. At the I/M editing site, the editing level increased gradually from 40% to 50% during aging. The increased level of editing was moderate between mice of 1.5-month and 12-month in age. However, there was a significant 5% increase in editing level observed in mice of 16-month over mice that were 1.5-month old (p=0.0132). When the mice reached 24-month in age, the editing level was increased by 10% (1.5 months *VS*. 24 months p=0.0185; 12

months *VS.* 24 months p=0.0130) (Figure 3.3 A). Similarly, the increase of editing level at the Y/C site occurred mainly between 12 and 16 months (1.5 months *VS.* 16 months p=0.0229, 12 months *VS.* 16 months p=0.0254) and then maintained at more than 30% between 16 to 24 months (Figure 3.3 B). These results showed that the level of RNA editing at the IQ-domain of $Ca_V1.3$ channels increased during aging. It seemed that the most significant increase occurred after the mice grew to 12 or 16 months in age.

Owing to the slower CDI of the edited channels, the elevated editing level would lead to an increased amount of Ca^{2+} flowing into the neurons, assuming there are no other changes. This increased Ca^{2+} influx will very likely affect the firing frequency of spontaneous action potentials in the pace-making neurons. However, as the increase in editing level is moderate, it brings out another question on how this slight increase in edited $Ca_V1.3$ channels could contribute to exacerbate oxidative stress in the ER and mitochondria (Chan, Gertler and Surmeier 2009, Chan et al. 2010). To address this question, further study is required to investigate the neurological effects of the increased editing level and the effects of increased Ca^{2+} influx on downstream signaling pathways in dopaminergic neurons. The $Ca_V1.3$ $ECS^{-/-}$ mouse would be a good animal model to study the role of RNA editing in IQ domain in motoric functions and to examine whether the abolishment of editing would be protective or detrimental to DA neurons in SN.

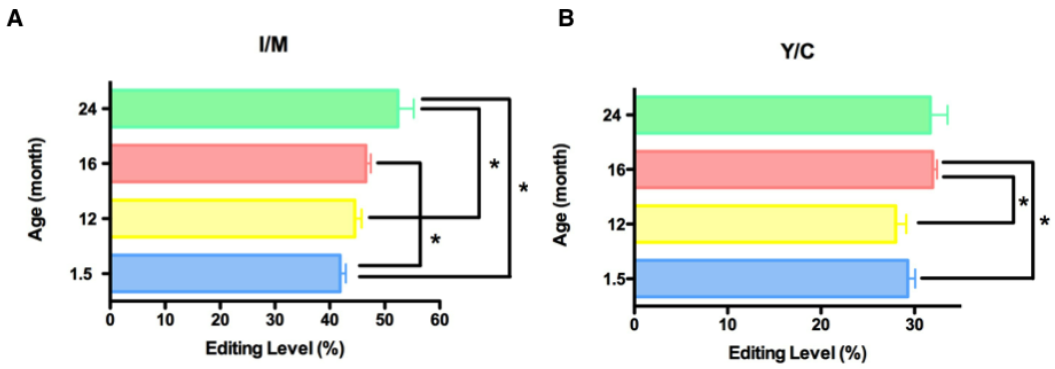

Figure 3.3 IQ-domain RNA editing level in substantia nigra during aging. A. I/M site RNA editing level evaluated at different age. B. Y/C site RNA editing level at different age. Student's T-test, two-tails, unpaired.

3.4 Level of IQ-domain RNA editing in suprachiasmatic nucleus changed in a circadian rhythmic manner

The pace-making activity has shown to be reduced in SCN neurons of ADAR2$^{-/-}$/GluR-B$^{R/R}$ mice corresponding with the total lack of editing of the $Ca_V1.3$ channels in these mice (Huang et al. 2012a). However, it was unknown whether IQ-domain editing is influenced by circadian rhythm according to the light-dark cycle, which might contribute to the diurnal regulation of Ca^{2+} current in SCN neurons (Pennartz et al. 2002). To this end, the SCN regions were collected at 8 time points across 24 hours from mice housed in 12 hour light-dark cycles.

The direct sequencing of the RT-PCR products amplified from the total RNA extracted from the SCN tissues revealed that the editing levels were generally higher during the day than at night (Figure 3.4 A). Specifically, the editing levels increased after the light-on time (ZT time 0). It reached the highest level of about 80% at ZT time 9 and then

decreased drastically thereafter. To serve as controls, tissues from the cortex were also collected from the same mice at the same time points. RNA editing of cortical tissues were maintained at almost constant levels throughout the whole day at both I/M and Y/C sites (Figure 3.4 B).

Importantly, the rhythmic variation of editing directly correlated with the circadian regulation of spontaneous firing frequency of SCN neurons. The higher editing level yields more edited channels with slower CDI, to allow more Ca^{2+} influx into the pace-making SCN neurons to therefore trigger higher frequency of spontaneous action potentials in the day. By contrast, at night, lower editing level results in lower Ca^{2+} influx and lower firing frequency. As rodents are nocturnal, the role of IQ-domain RNA editing in pace-making activity of neurons in SCN and its effect on physiological and behavioral circadian rhythm is therefore worth investigating. As discussed previously, the $ADAR2^{-/-}$ /GluR-$B^{R/R}$ mouse was not a perfect model to study IQ-domain RNA editing of $Ca_V1.3$. The influence of editing on SCN pace making activity would therefore be better validated in the $Ca_V1.3$ $ECS^{-/-}$ mice where RNA editing of $Ca_V1.3$ channel is eliminated. Furthermore, circadian rhythm related behavioral study like the running wheel test could be performed using such $Ca_V1.3$ $ECS^{-/-}$ mice to show the effect of RNA editing has on circadian rhythm related behaviors.

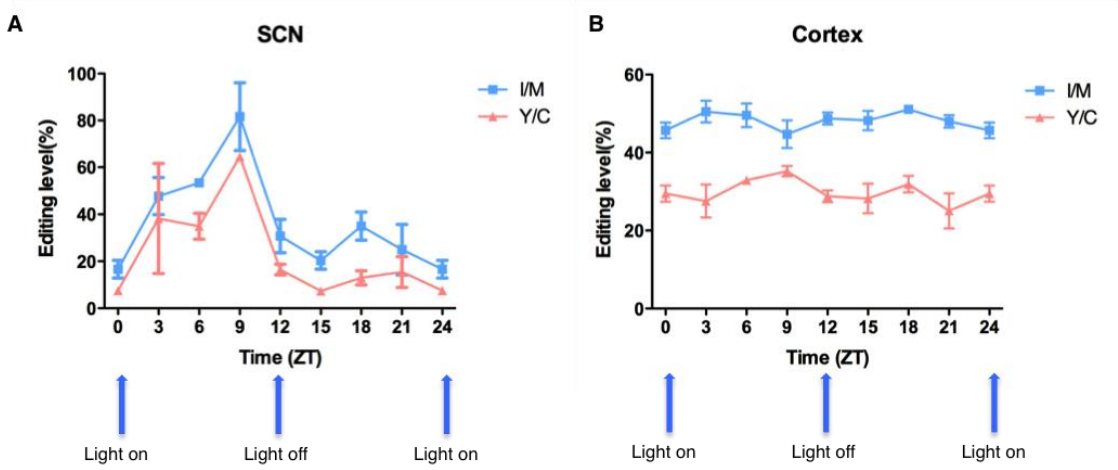

Figure 3.4 IQ-domain RNA editing regulated in suprachismatic nucleus with circadian rhythm. A. IQ-domain RNA editing was circadian rhythmically regulated in SCN. B: IQ-domain RNA editing maintained at almost the same across 24 hours in cortex. Blue arrow: time for light on/off.

3.5 No difference in editing level detected in a mouse model of depression

$Ca_V1.3$ channel has been shown to be involved in mood disorders (Busquet et al. 2010). However, whether IQ-domain RNA editing is altered under mood disorder conditions is still largely an open question. To address this question, R439H_TPH2KI mice was used as a mouse model of depression to determine whether the level of RNA editing is altered. Serotonin deficiency was found in depression. Loss of function SNP in human tryptophan hydroxylase 2 (*hTPH2*), the rate-limiting enzyme in serotonin synthesis, was reported in patients with unipolar major depression (Zhang et al. 2005b). The TPH2KI mice introduced a loss of function mutation R439H resulting in serotonin deficiency. Depression-like behaviors were observed during phenotyping (Jacobsen, Medvedev and Caron 2012, Beaulieu et al. 2008).

In this study, brain tissues of the amygdala and hippocampus regions were collected from both TPH2KI and TPH2WT mice. Direct DNA sequencing of the RT-PCR products showed that the RNA editing level was comparable in TPH2KI and the wild-type littermate mice (Figure 3.5). Although it seemed that in hippocampus, the editing level was slightly lower at both I/M and Y/C sites in the KI mice than WT mice, the difference was not statistically significant. As the antidepressant-like behavior in the $\alpha 1D^{-/-}$ mice suggested a potential role of $Ca_V1.3$ channel in depression, one possible explanation is that the depression-liked behavior observed in the TPH2KI mice is mainly a genetic defect resulting in altered level of serotonin production. The serotonin deficiency related depression behavior might not directly affect the RNA editing process of $Ca_V1.3$ transcripts. As such results from this model of depression alone cannot rule out the possible association between IQ-domain RNA editing and depression, further investigations are required to unveil the role of IQ-domain editing in depression.

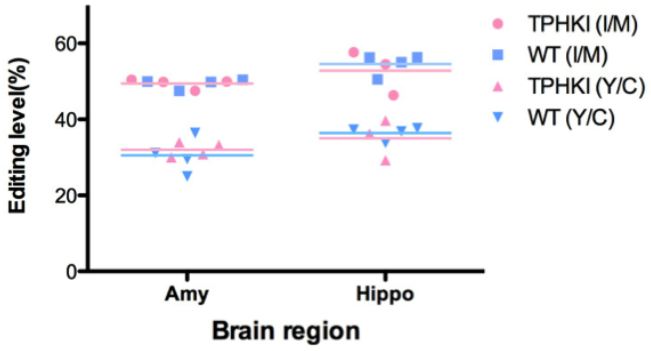

Figure 3.5 IQ-domain RNA editing in mouse depression model. No significant difference of RNA editing at I/M or Y/C site was detected in neither amygdala nor hippocampus. Student's T-test, two-tails, unpaired.

3.6 Knockdown of RNA editing of $Ca_V1.3$ channels by antisense oligonucleotides

A-to-I RNA editing requires the pre-mRNA substrates to form a double stranded hairpin structure for recognition and binding by ADARs. As predicted by Mfold on web server (http://mfold.rna.albany.edu), there is an imperfect double stranded hairpin structure formed between exon 41 that encodes the IQ domain and the intronic ECS found within intron 40.

To validate the predicted hairpin structure and identify the exact ECS that is critical for RNA editing to occur, antisense oligonucleotides knockdown experiments were performed. Three 20-nt antisense oligonucleotides (ASOs) targeting to the ECS and its upstream or downstream sequence were designed to test whether disruption of the stem-loop structure may reduce editing level. Based on the predicted hairpin structure, a mini-gene named pRK5-gIQECS was constructed that contained the ECS, IQ domain and the intervening intronic sequences (provided by Dr. Huang Hua). Significant editing level was observed in this mini-gene when cotransfected with ADAR2 (Huang et al. 2012a). In this study, mini-gene pRK5-gIQECS, pIRES2-AcGFP1-ADAR2 and ASOs were cotransfected into HEK 293 cells and we evaluated whether the ASOs could disrupt the hairpin structure by determining the editing levels of the IQ domain (Figure 3.6 B).

ASO that covered the entire ECS (Figure 3.6 A) reduced the editing level of the IQ domain found in the mini-gene to 60% at I/M and 70% at Y/C site (Figure 3.6 C). While the other two ASOs (ASO I and ASO II) targeting to either upstream or down stream of ECS did not have the knockdown effect (Figure 3.6 C). The comparison of editing level was conducted with the normalized editing level with control oligonucleotide. The results suggest strongly the importance of the hairpin structure for RNA editing of $Ca_V1.3$ IQ-domain. Moreover, the identification of ECS provided important guidance for the generation of $Ca_V1.3$ $ECS^{-/-}$ mice.

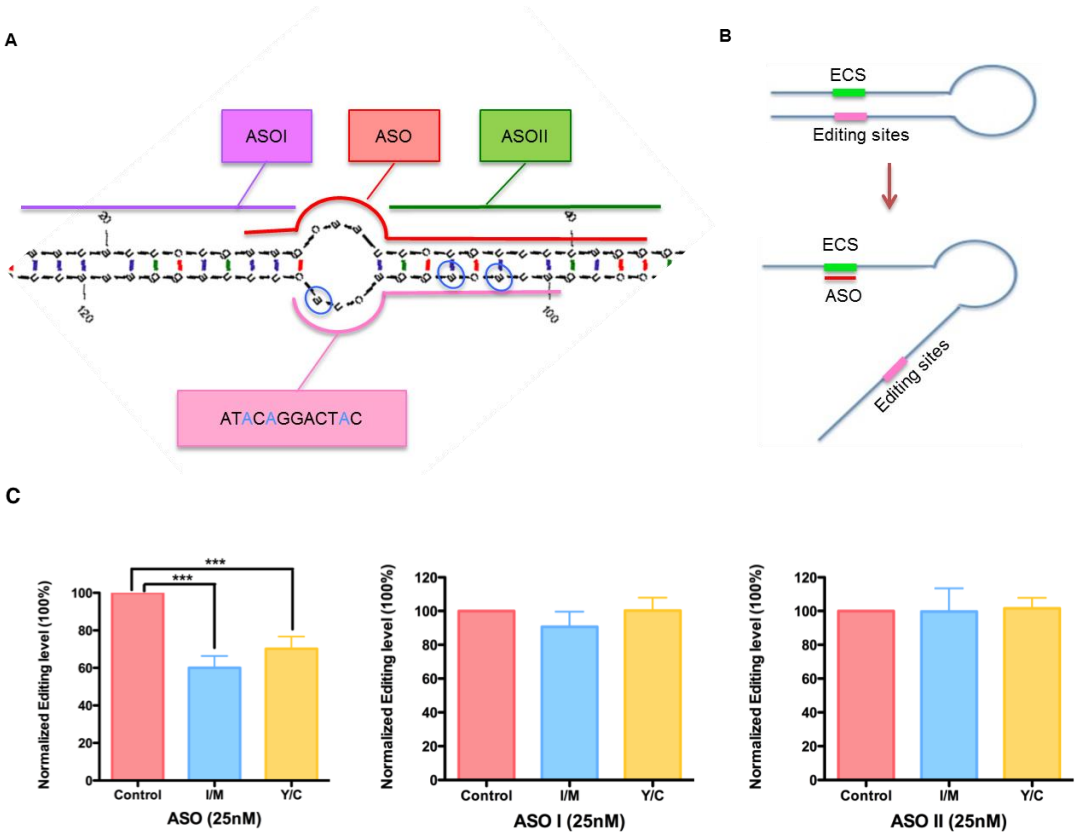

Figure 3.6 Antisense Oligo knockdown of IQ-domain RNA editing in mini-gene. A. Double strand hairpin structure predicted by Mfold, dG=-59.10. Pink line: editing site sequence (pink box), the three editing site are circled and labled in blue. Red line: ASO targeting sequence. Purple line: ASOI targeting sequence. Green line: ASOII targeting sequence. B. Schematic diagram

showing the disruption of hairpin structure by competitive binding of ASO onto the ECS. C. ASOs knockdown of editing level at both I/M and Y/C sites comparing to the control oligo. Left, Reduced editing level at both I/M and Y/C sites by 25 nM ASO ($p<0.01$, n=6). Middle, no significant change of editing level with co-transfection of 25 nM ASO I (n=3). Right, no significant change of editing level with co-transfection of 25 nM ASO II (n=3)

3.7 Generation of $Ca_V1.3$ $ECS^{-/-}$ mice

As presented previously, the level of IQ-domain RNA editing was altered under different physiological conditions such as an increase in aging in substantia nigra, and modulation in a circadian rhythmic fashion in suprachiasmatic nucleus. There are therefore compelling reasons to investigate the functional and physiological roles of $Ca_V1.3$ IQ-domain editing in a more comprehensive manner. Based on the results of ASO knockdown that the ECS was confirmed to be essential for RNA editing of IQ domain to occur, global ECS knockout mice were generated.

First, long-form and short-form targeting constructs were generated. The long-form targeting construct contained 4 kb of genomic sequences upstream of the ECS and 4 kb of genomic sequences downstream of the ECS with the neomycin cassette replacing the ECS. It was used to optimize the genotyping conditions for both PCR screening and southern blot analyses, and to serve as positive control in the genotyping experiments. The short-form construct contained 4 kb of genomic sequences upstream of the ECS and 1 kb of genomic

sequences downstream of ECS with the neomycin cassette replacing the ECS (Figure 3.7.1). This construct was transfected into ES cells to allow homologous recombination to occur. The transfected ES cells were first selected by applying G418 and approximately 300 ES colonies were then picked for PCR screening (Figure 3.7.2 A) and southern blot analysis (Figure 3.7.2 B). Only one clone (IC10) was confirmed to have undergone homologous recombination successfully.

Second, the positive ES clone was then microinjected into C57BL/6 blastocysts. Among the 55 injected embryos, 28 of the F0 pups were chimeras with agouti color. F0 males were crossed with C57BL/6 females to generate the F1 generation. The F1 mice were genotyped by both PCR screening (Figure 3.7.2 C) and southern blot analysis (Figure 3.7.2 D). Male and female F1 mice with Neo/WT genotype were selected for breeding to generate the ECS-null mice (F2).

Third, ECS-null mice were then crossed with Actin-Cre mice to delete the selection marker Neo cassette. F3 $ECS^{-/WT}$ mice were crossed with C57BL/6 to confirm the whole body deletion of Neo cassette (F4). The $ECS^{-/-}$ mice (F5) were obtained by crossing the male and female heterozygous F4 mice. The genotypings were performed by both PCR screening (Figure 3.7.2 E) and southern blot analysis (Figure 3.7.2 F).

Fourth, the $Ca_V1.3$ $ECS^{-/-}$ mice are undergoing backcross with C57BL/6 mice for 6-10 generations before we conduct more behavioral studies.

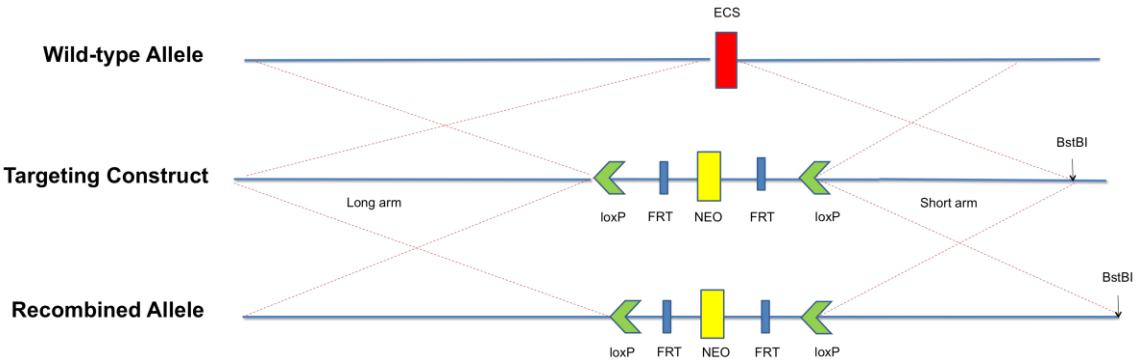

Figure 3.7.1 Schematic graph of $Ca_V1.3$ $ECS^{-/-}$ mice generation strategy. Homologous recombination between targeting construct and wild type allele replaced ECS with Neo cassette to generate recombined allele.

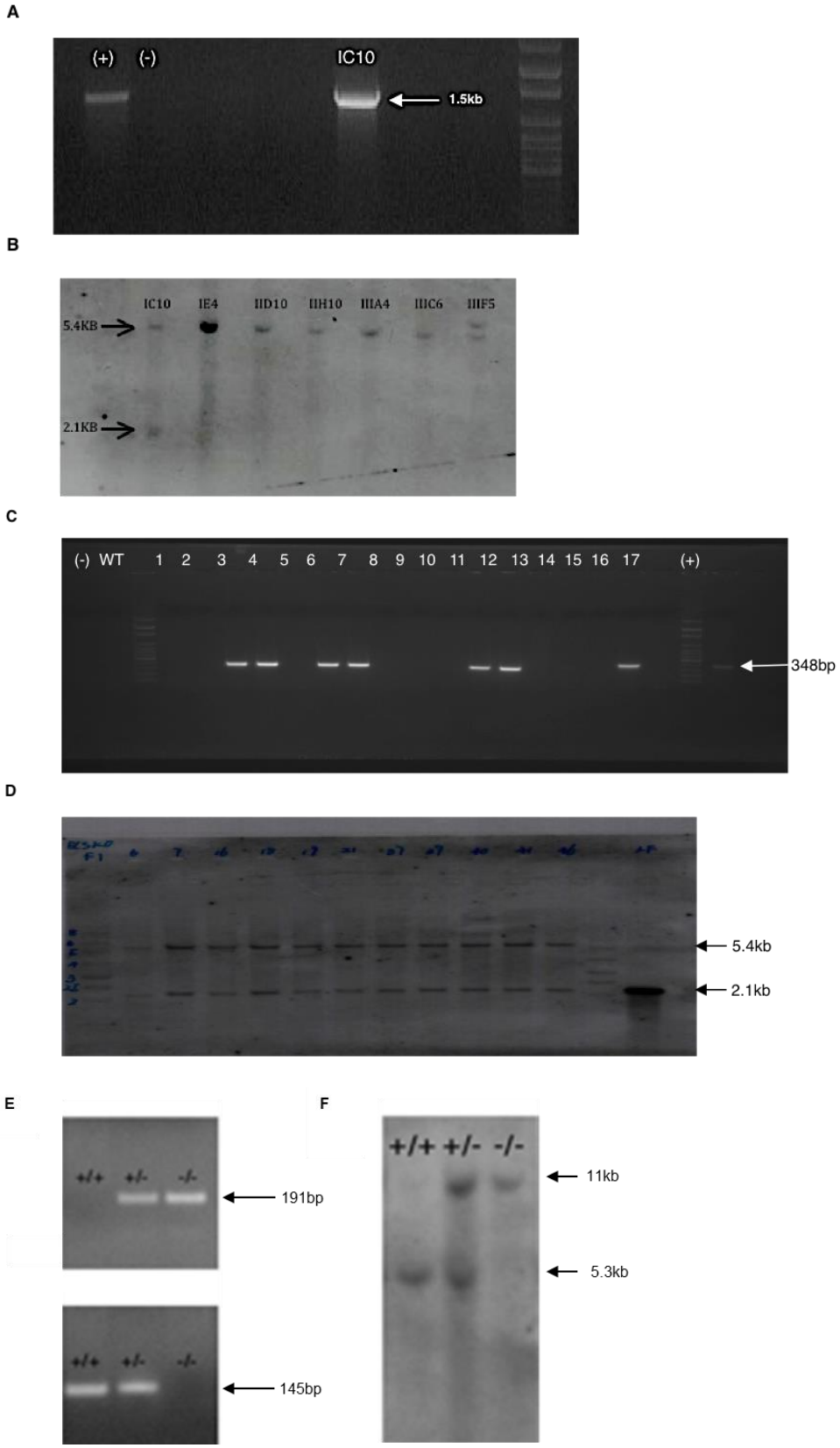

Figure 3.7.2 Genotyping to identify ES cells and mice with desired genotype. A. PCR screening of ES colonies. 1.5 kb band indicated positive homologous

recombination. B. Southern blot analysis of ES colonies. 5.4 kb band indicated the wild type allele; 2.1 kb band indicated the replacement of Neo cassette to ECS. C. PCR genotyping of F1 mice. 348bp band indicated heterozygous genotype. D. Southern blot analysis of F1 mice. Appearance of both 5.4 kb and 2.1 kb bands indicated the heterozygous genotype. E. PCR genotyping of F5 mice. Upper panel: 191 bp band indicated knockout allele; lower panel: 145 bp band indicated wild type allele. F. Southern blot analysis of F5 mice. 11 kb band indicated wild type allele, while 5.3 kb band indicated knockout allele.

3.8 Abolished RNA editing in $Ca_V1.3$ $ECS^{-/-}$ mice with similar transcript and protein expression levels, and C-terminal splicing pattern

To characterize the $Ca_V1.3$ $ECS^{-/-}$ mice, the editing levels of the IQ-domain were first evaluated. The direct DNA sequencing results of the RT-PCR products from whole brain total RNA revealed that RNA editing of the IQ-domain was totally abolished in $Ca_V1.3$ $ECS^{-/-}$ mice, and the editing level in $Ca_V1.3$ $ECS^{+/-}$ mice was about half of the level detected in $Ca_V1.3$ WT littermates (Figure 3.8 A and B). These results clearly demonstrated that the ECS was essential for RNA editing, and the deletion of the ECS could totally abolish editing of the $Ca_V1.3$ IQ-domain.

Second, the transcription levels of *Cacna1d* in the whole brain were compared between $Ca_V1.3$ $ECS^{-/-}$ and $Ca_V1.3$ WT mice by using real-time PCR method. The relative transcription level (ΔC_T) showed no

difference (Figure 3.8 C), which indicated that the deletion of ECS did not affect the level of *Cacna1d* transcripts expressed in the brain.

Third, the protein expression level was also evaluated by western blot analyses. Whole brains from both $Ca_V1.3$ ECS$^{-/-}$ and $Ca_V1.3$ WT mice were obtained for the evaluation of $Ca_V1.3$ protein expression level. The expression level was detected by western blot with pAb_$Ca_V1.3_{42}$ antibody (Tan et al. 2011). Three mouse brains from each group were obtained and processed at the same time on same blot for detection of $Ca_V1.3$ protein expression. Although individual difference occurred between samples from same genotype (Figure 3.8 D), after normalizing with the expression level of Actin, in line with the transcription levels of *Cacna1d*, there was no difference in average $Ca_V1.3$ expression level between $Ca_V1.3$ ECS$^{-/-}$ and $Ca_V1.3$ WT mice (Figure 3.8 E).

Fourth, as the C-terminus of $Ca_V1.3$ channel undergoes multiple alternative splicing events, the splicing pattern of the C-terminus was compared between $Ca_V1.3$ ECS$^{-/-}$ and $Ca_V1.3$ WT to examine whether it changed upon the deletion of the intronic ECS. Alternative splicing occurring within exons 40 to exon 48 were examined (Figure 3.8 F). The results revealed that the splicing pattern was the same in the $Ca_V1.3$ ECS$^{-/-}$ as it was in the $Ca_V1.3$ WT mice (Figure 3.8 G). These results indicated that the deletion of ECS did not affect the splicing pattern in the C-terminus of $Ca_V1.3$ channels.

In summary, the $Ca_V1.3$ ECS$^{-/-}$ mice showed nearly no RNA editing in the IQ-domain of $Ca_V1.3$ channels, while the transcription level, protein expression and C-terminal splicing were similar as compared to the $Ca_V1.3$ WT.

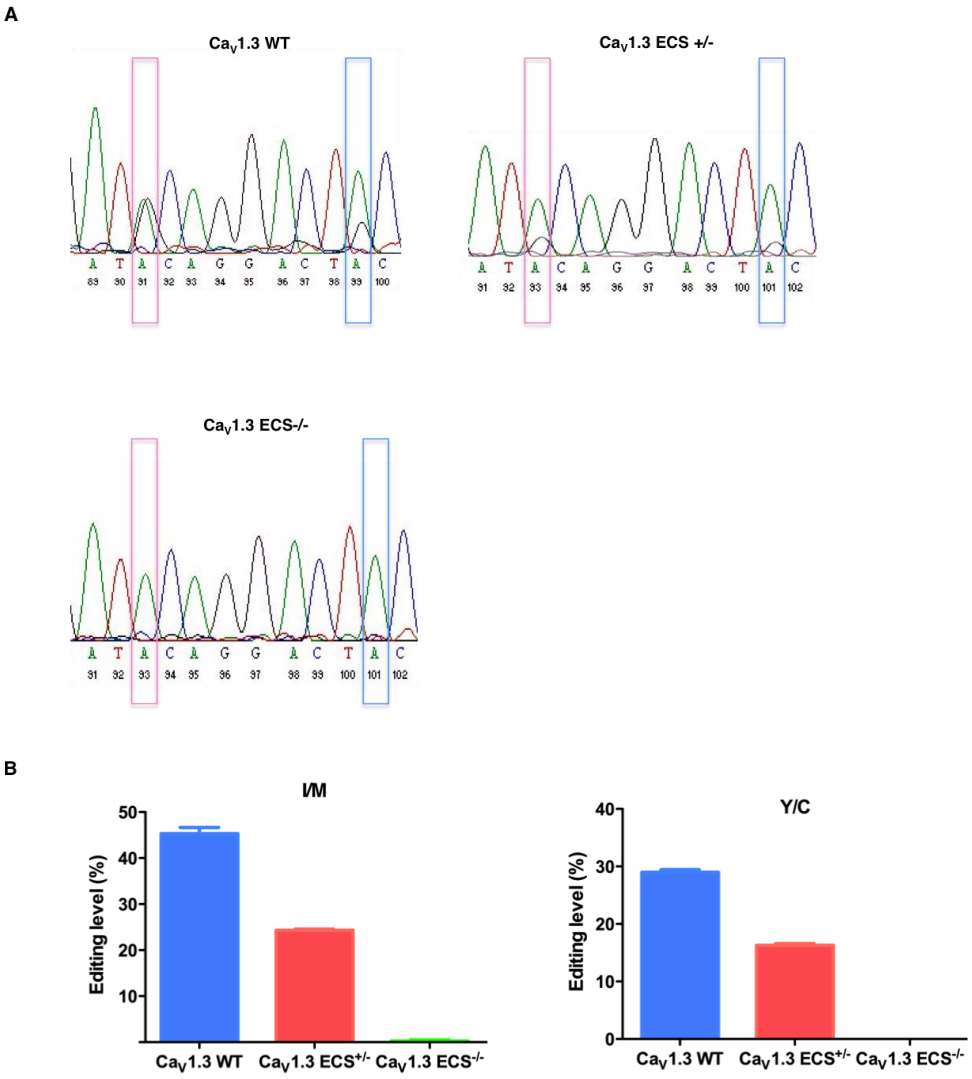

C

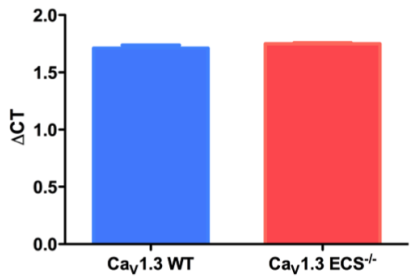
2.0
1.5
1.0
0.5
0.0
ΔCT
CaV1.3 WT
CaV1.3 ECS-/-

D

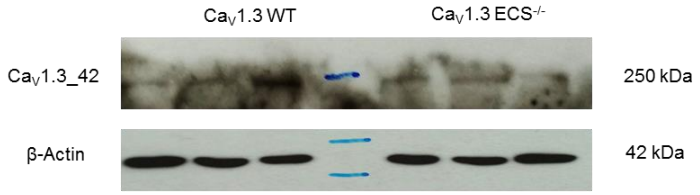
CaV1.3 WT
CaV1.3 ECS-/-
CaV1.3_42
250 kDa
β-Actin
42 kDa

E

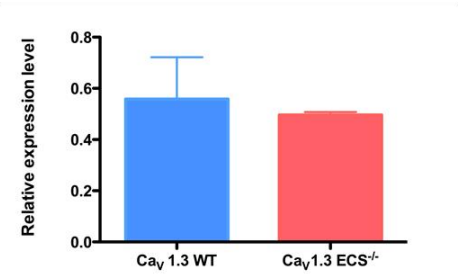
0.8
0.6
0.4
0.2
0.0
Relative expression level
CaV 1.3 WT
CaV1.3 ECS-/-

F

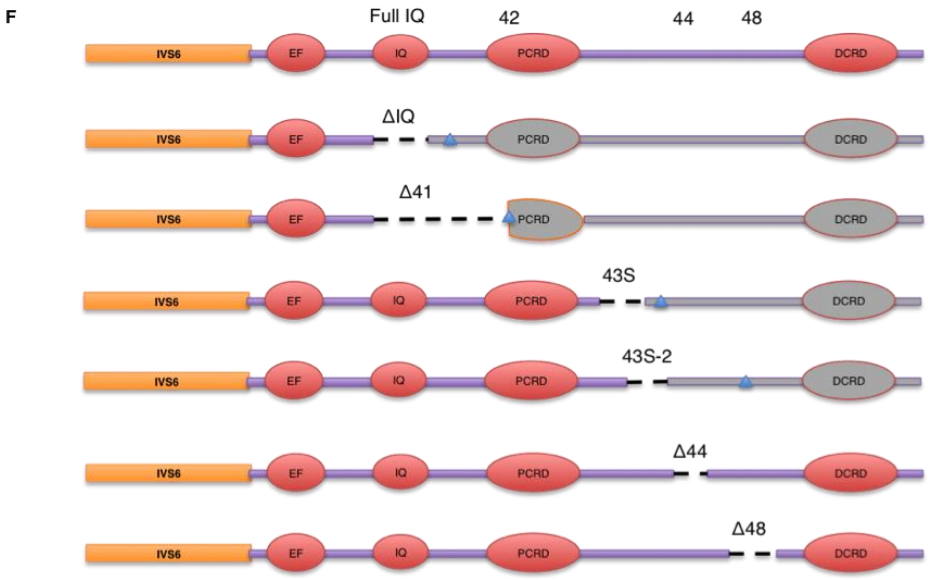
Full IQ
42
44
48
IVS6
EF
IQ
PCRD
DCRD
ΔIQ
Δ41
43S
43S-2
Δ44
Δ48

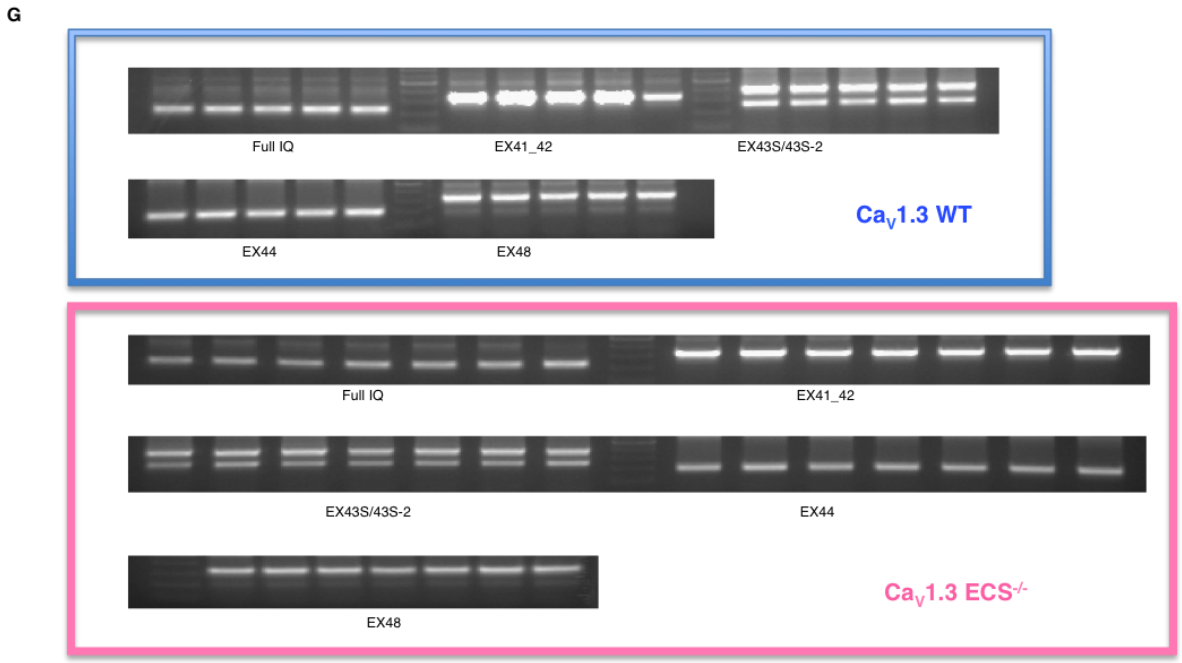

Figure 3.8 Molecular characterizations of $Ca_V1.3$ $ECS^{-/-}$ mice. A. Electropherograms showing editing level of whole brain in $Ca_V1.3$ WT, $Ca_V1.3$ $ECS^{+/-}$ and $Ca_V1.3$ $ECS^{-/-}$ mice. B. Statistical analysis of editing level. RNA editing level in $Ca_V1.3$ $ECS^{+/-}$ mice (n=6) was half of the level in $Ca_V1.3$ WT (n=6) at both I/M and Y/C sites, while in $Ca_V1.3$ $ECS^{-/-}$ mice RNA editing in IQ domain of $Ca_V1.3$ was totally abolished (n=6). C. Transcription level of *Cacna1d* in $Ca_V1.3$ WT and $Ca_V1.3$ $ECS^{-/-}$ mice. The relative expression level was represented by ΔC_T after normalizing to the β-actin internal control. D. Representative immunoblot showing $Ca_V1.3$ channel expression level in $Ca_V1.3$ WT (n=3) and $Ca_V1.3$ $ECS^{-/-}$ (n=3) mice detected in western blot analysis, whereas β-actin was used as input control. E. Relative expression level of $Ca_V1.3$ channel presented by the average level after normalizing to the level of β-actin. F. Schematic diagram of C-terminal alternative splicing variants. Upper panel, transmembrane pore-forming structure of α1D subunit. Lower panel, splice variants generated by alternative splicing in C-terminus. G. C-terminal alternative splicing pattern in $Ca_V1.3$ WT (n=5) and $Ca_V1.3$ $ECS^{-/-}$ (n=7) mice. $Ca_V1.3$ WT and $Ca_V1.3$ $ECS^{-/-}$ mice showed similar splicing

pattern: full IQ, EX41_42, EX43S/EX43-S2, EX44 and EX48. Blue triangle: stop codon.

3.9 Lower frequency of spontaneous firing of action potentials of SCN neurons in $Ca_V1.3$ $ECS^{-/-}$ mice

As presented previously, IQ-domain RNA editing of $Ca_V1.3$ was modulated in a circadian rhythmic manner in SCN neurons. Therefore, it would be interesting to investigate the spontaneous firing of pace making neurons in this region. In the $ADAR2^{-/-}$/GluR-$B^{R/R}$ mice, lower firing frequency was observed as compared to wild type mice (Huang et al. 2012a). To test whether eliminating specifically IQ-domain RNA editing has similar effect on pace making activity of SCN neurons, whole cell patch clamp recording was performed on SCN brain slices from both $Ca_V1.3$ $ECS^{-/-}$ and $Ca_V1.3$ WT mice. The brain slices were obtained at ZT4-5. And patch clamp electrophysiological recordings were performed during ZT6-10.

In line with the findings in previous study, the spontaneous firing frequency in SCN neurons of $Ca_V1.3$ $ECS^{-/-}$ mice was lower than it was in $Ca_V1.3$ WT mice (Figure 3.9 A and B). Due to the time limitation, only two recordings from each genotype were obtained. Nevertheless, the results showed obvious trend of lower firing frequency in $Ca_V1.3$ $ECS^{-/-}$ mice. It indicated that with deletion of IQ-domain RNA editing, only unedited channels were present in these pace making neurons. As unedited channels exhibited faster CDI a lower firing frequency of

spontaneous action potentials was expected and observed. This part of work is still ongoing. More recordings would be needed to confirm the present trend. Detailed analysis of the Ca^{2+} spikes under the spontaneous firing would also be performed to determine the effects of IQ domain RNA editing on Ca^{2+} influx in pace making neurons.

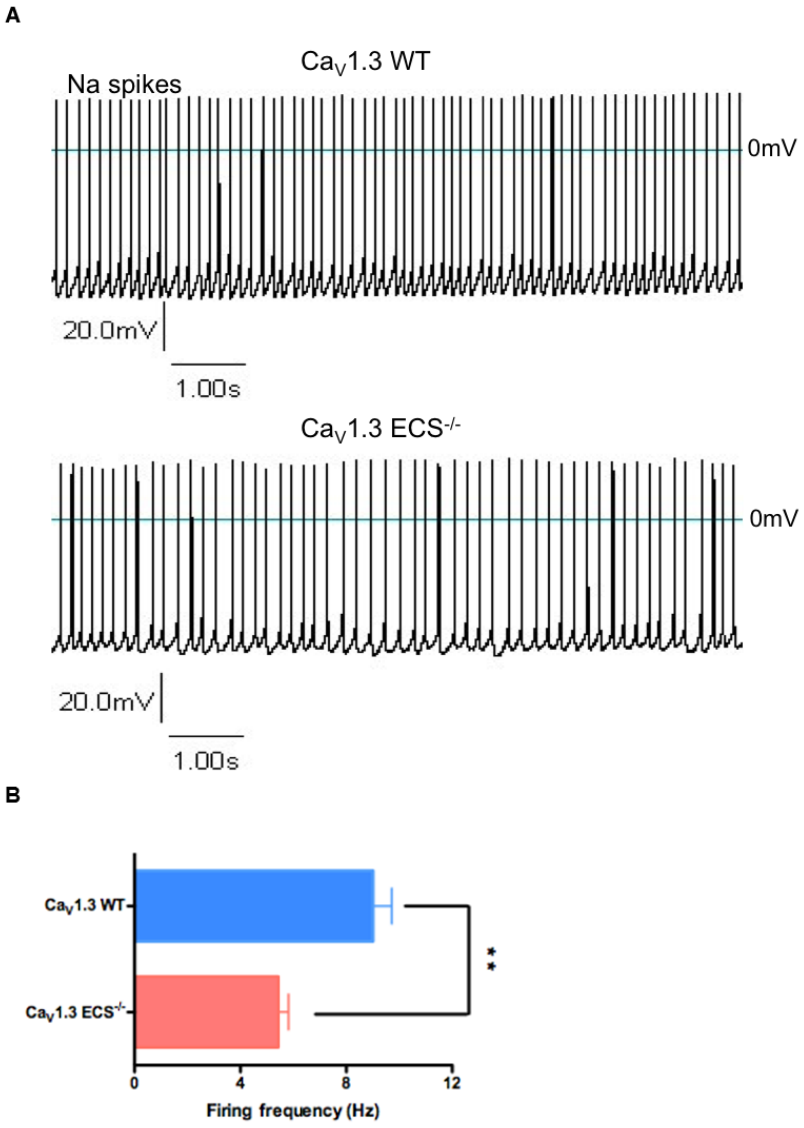

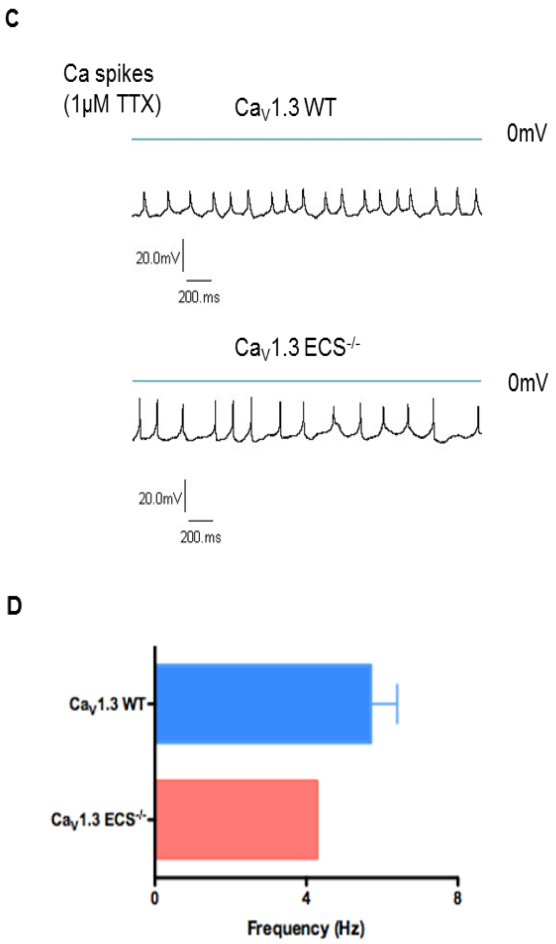

Figure 3.9 Comparison of pace making activity in SCN neurons between $Ca_V1.3$ WT and $Ca_V1.3$ $ECS^{-/-}$ mice. A. Na spikes in SCN neurons of $Ca_V1.3$ WT (upper panel) and $Ca_V1.3$ $ECS^{-/-}$ (lower panel). B. Average firing frequency of spontaneous action potentials in $Ca_V1.3$ WT (n=7) and $Ca_V1.3$ $ECS^{-/-}$ mice (n=6). C. Calcium spike in SCN neurons of $Ca_V1.3$ WT (upper panel) and $Ca_V1.3$ $ECS^{-/-}$ (lower panel). D. Average frequency of underlying calcium spike in $Ca_V1.3$ WT (n=2) and $Ca_V1.3$ $ECS^{-/-}$ mice (n=1).

3.10 Anxiety-like behavior and disrupted circadian rhythm in $Ca_V1.3$ $ECS^{-/-}$ mice

The role of $Ca_V1.3$ channel in mood disorder, the circadian rhythmic modulation of RNA editing of the IQ-domain observed in SCN and the

increased editing level in SN during aging had been discussed in the previous chapter. Therefore, the physiological and behavioral changes arising from abolishment of RNA editing would be interesting to investigate. Several behavioral tests were performed for preliminary behavioral characterization of the $Ca_V1.3$ $ECS^{-/-}$ mice, elevated zero maze was used to assess their anxiety levels, while rota-rod and balance beam tests were used to examine the motor functions, and running wheel in home-cage test was used to evaluate their circadian rhythms.

First, $Ca_V1.3$ $ECS^{-/-}$ mice showed higher level of anxiety as the time they spent on the open arms of the elevated zero maze was approximately 50% less than $Ca_V1.3$ WT (Figure 3.10 C, $p=0.0193$; $n=5$). As they tended to stay in the close arm, the frequency of transition and total distance traveled during the test were also about half of what were observed in $Ca_V1.3$ WT mice (Figure 3.10 A and B). $Ca_V1.3$ $ECS^{-/-}$ mice spent about 2-fold more time on the balance beam on Day 1 (Figure 3.10 D, $p<0.001$, $n=5$) and this result suggests that they were more anxious. As for depression, although no alteration of RNA level editing was detected in the TPH2KI depression mouse model, depression related behavioral test like forced swimming test and tail suspension test would be conducted to determine whether elimination of IQ-domain RNA editing might affect depression-like behaviors.

Second, the motor function of $Ca_V1.3$ $ECS^{-/-}$ mice seemed to be unaffected in the behavioral tests. On one hand, although the time $Ca_V1.3$ $ECS^{-/-}$ mice took to cross the beam was significantly longer than $Ca_V1.3$ WT on Day 1, surprisingly after a two-day gap, their performance improved drastically to the same level as $Ca_V1.3$ WT in the following two days of tests (Figure 3.10 D). However, the number of foot slips showed that the $Ca_V1.3$ WT mice improved their balancing on the beam during the three days from average 4 foot slips to almost no foot slip, while for $Ca_V1.3$ $ECS^{-/-}$ mice in spite of improving performance, they still had more foot slips on the beam than $Ca_V1.3$ WT (Figure 3.10 E). On the other hand, the learning curve for the rota-rod test suggested that the $Ca_V1.3$ $ECS^{-/-}$ mice were able to learn and improve their motor coordination as same as $Ca_V1.3$ WT mice (Figure 3.10 F). These results indicate that the $Ca_V1.3$ $ECS^{-/-}$ mice showed slightly impaired balancing ability, but it did not affect their overall motor function.

Third, $Ca_V1.3$ $ECS^{-/-}$ mice showed disrupted circadian rhythm as assessed in the running wheel test. The activities of mice on the running wheel as well as in the homecages were recorded over 48 hours. The results show that $Ca_V1.3$ $ECS^{-/-}$ mice spent 5-fold more time on the running wheel during the day time (ZT1-12) than $Ca_V1.3$ WT, while during the night (ZT13-24), they seemed to be slightly less active than $Ca_V1.3$ WT mice (Figure 3.10 G). The overall activity of $Ca_V1.3$ $ECS^{-/-}$ mice on running wheel was also higher than WT mice

(Figure 3.10 H). This indicates that $Ca_V1.3$ $ECS^{-/-}$ mice had higher activity and disrupted sleep pattern during the day when they were supposed to be sleeping. As discussed in the previous chapter, RNA editing of the IQ-domain was regulated in a circadian rhythmic fashion, which was higher during the day than night. The lower firing frequency observed in $Ca_V1.3$ $ECS^{-/-}$ mice during the day-time is possibly due to reduced Ca^{2+} influx into pace-making neurons caused by abolished RNA editing. Therefore, the higher activity observed during the day might be explained by the reduced Ca^{2+} influx and firing frequency of spontaneous action potentials. However, the mechanism of how the pace-making activity controls the output of physiological and behavioral circadian rhythm is still largely unknown.

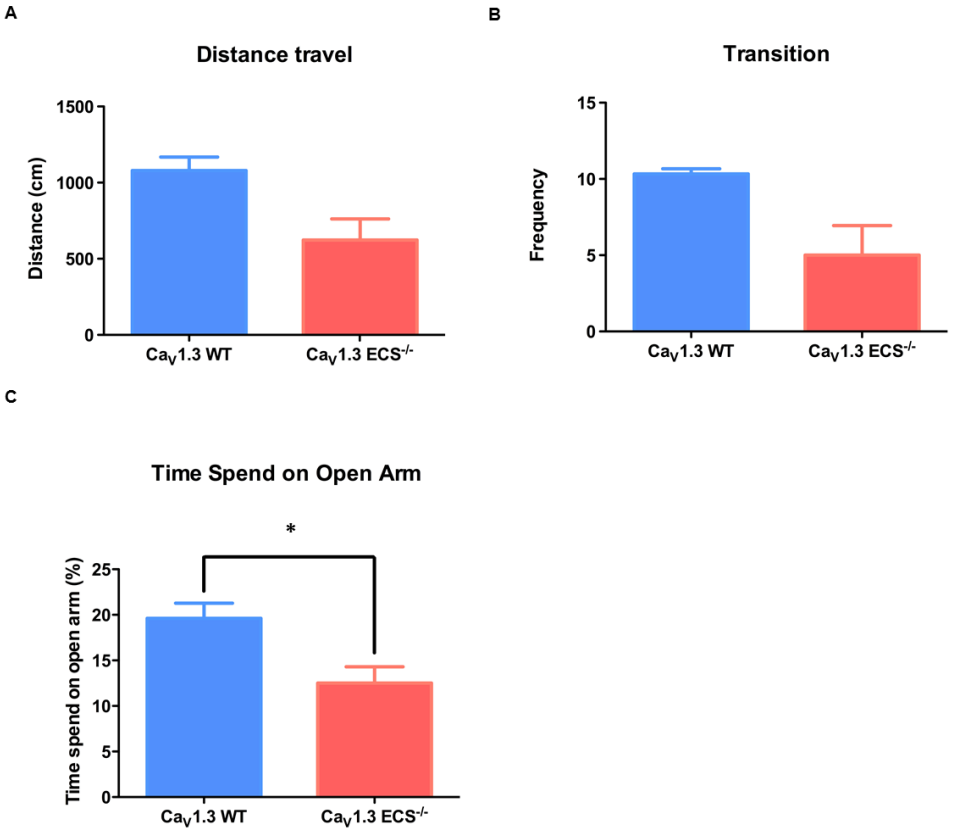

D

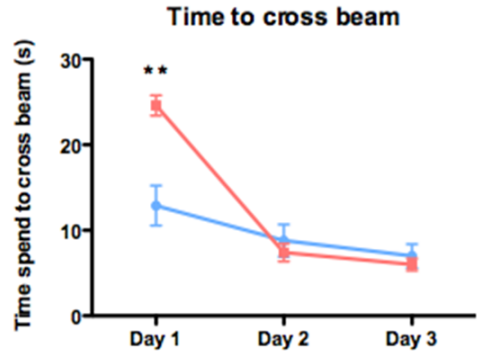
Time to cross beam
Time spend to cross beam (s)
30
20
10
0
**
Day 1
Day 2
Day 3

E

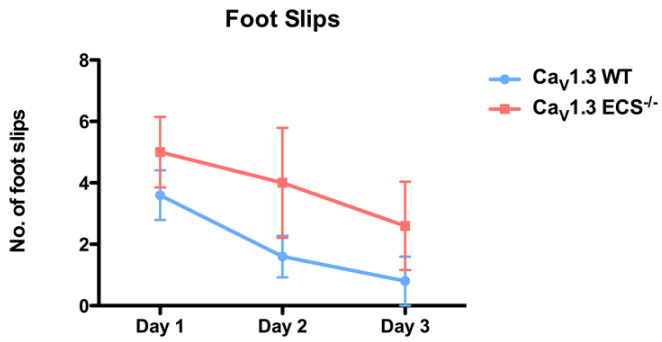
Foot Slips
No. of foot slips
8
6
4
2
0
Day 1
Day 2
Day 3
Ca$_V$1.3 WT
Ca$_V$1.3 ECS$^{-/-}$

F

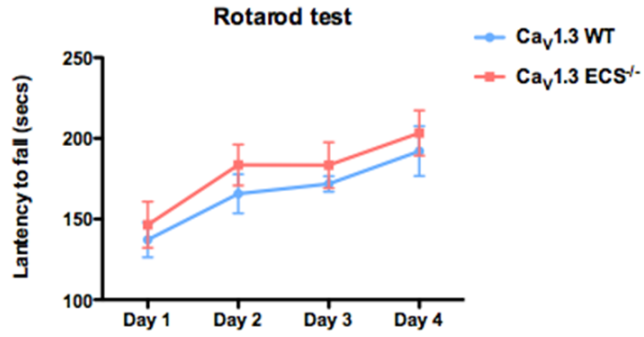
Rotarod test
Latency to fall (secs)
250
200
150
100
Day 1
Day 2
Day 3
Day 4
Ca$_V$1.3 WT
Ca$_V$1.3 ECS$^{-/-}$

G

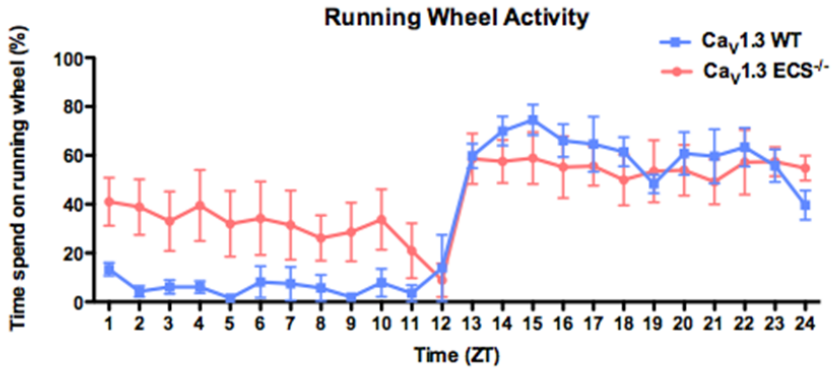
Running Wheel Activity
Time spend on running wheel (%)
100
80
60
40
20
0
1 2 3 4 5 6 7 8 9 10 11 12 13 14 15 16 17 18 19 20 21 22 23 24
Time (ZT)
Ca$_V$1.3 WT
Ca$_V$1.3 ECS$^{-/-}$

H

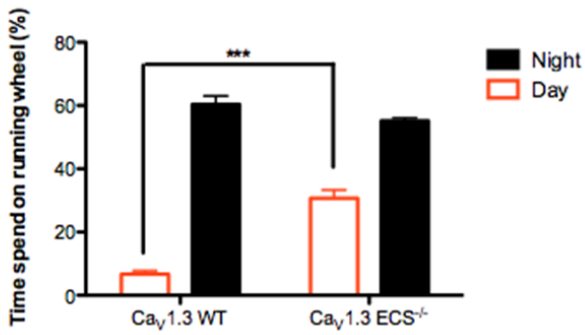
Time spend on running wheel (%)
80
60
40
20
0
***
Night
Day
Ca$_V$1.3 WT
Ca$_V$1.3 ECS$^{-/-}$

Figure 3.10 Performance of $Ca_V1.3$ $ECS^{-/-}$ and $Ca_V1.3$ WT mice in behavior tests. A. Frequency of transition on elevated zero maze. On average $Ca_V1.3$ $ECS^{-/-}$ mice showed half of the transition frequency compared to $Ca_V1.3$ WT mice. B. Distance traveled on elevated zero maze. On average $Ca_V1.3$ $ECS^{-/-}$ mice traveled half the distance traveled by $Ca_V1.3$ WT mice. C. Percentage of time spent on the open arm on elevated zero maze. $Ca_V1.3$ $ECS^{-/-}$ mice (12.50±1.79) spent significantly less time on the open arm compared to $Ca_V1.3$ WT mice (19.62±1.65) ($p=0.0193$, $n=5$) D. Learning curve of time spend on balance beam. $Ca_V1.3$ $ECS^{-/-}$ mice spent significantly longer time (24.60±1.177 sec) to cross the balance beam compared to $Ca_V1.3$ WT mice (12.90±2.342 sec) on Day1 ($p<0.001$, $n=5$). E. Learning curve of number of foot slips when walking across the balance beam. $Ca_V1.3$ WT mice had significantly less foot slips on day3 (0.8±0.8) than day1 (3.6±0.8124)($p=0.0396$, $n=5$), while the improvement of $Ca_V1.3$ $ECS^{-/-}$ mice is not significant. F. Learning curve of latency to fall on the rota-rod. The performance of $Ca_V1.3$ $ECS^{-/-}$ mice was slight better than $Ca_V1.3$ WT on the rota-rod, although they both improved during the four days. G. Running wheel activity across 24 hours. $Ca_V1.3$ $ECS^{-/-}$ mice spent significantly more time on the running wheel in the day (30.70±2.577%) than $Ca_V1.3$ WT mice (6.674±1.123%) ($p<0.001$, $n=5$). H. Overall activity on running wheel in day and night. $Ca_V1.3$ $ECS^{-/-}$ mice showed higher activity on running wheel than $Ca_V1.3$ WT mice ($p<0.001$, $n=5$).

3.11 Conclusion

This study has provided valuable insights into RNA editing in IQ-domain of $Ca_V1.3$ under certain physiological and disorder conditions. The editing level was modulated in a circadian rhythmic manner in

SCN and increased in SN during aging. Moreover, reduced firing frequency and disrupted circadian rhythm observed in $Ca_V1.3$ $ECS^{-/-}$ mice further indicated that IQ-domain RNA editing may be part of the underlying mechanism regulating the open properties of $Ca_V1.3$ channels and neuronal activities. Besides, the anxiety-like behavior of $Ca_V1.3$ $ECS^{-/-}$ mice suggested the functional role of RNA editing in anxiety. It is also possible that targeting modulation of RNA editing of $Ca_V1.3$ could potentially be helpful in clinical management of disease and disorders like anxiety, sleeping disorders and Parkinson's disease.

Chapter 4

Discussion

4.1 Deletion of ECS from mouse genome totally eliminated IQ domain RNA editing without affecting expression level of Cacna1d and C-terminal alternative splicing.

To evaluate the physiological roles of $Ca_V1.3$ IQ-domain RNA editing, an animal model would be needed. The current available model is the ADAR2$^{-/-}$/GluR-B$^{R/R}$ mouse, in which the gene encoding the RNA editing enzyme ADAR2 was deleted. As ADAR2 has several other substrates besides $Ca_V1.3$ channel such as Kv1.1 channel, GluR-B receptor and 5HT-2C receptor (Berg and Bush 2001, Miyoko et al. 1993, Bhalla et al. 2004), the ADAR2$^{-/-}$/GluR-B$^{R/R}$ mouse is therefore not an ideal model to interrogate the physiological roles of $Ca_V1.3$ IQ-domain RNA editing. In order to derive a better mouse model, $Ca_V1.3$ ECS$^{-/-}$ mice were generated. Before starting to generate the knockout mice, the identity and validation of the ECS were first done via using the ASO knockdown strategy.

Only the ASO covering all three editing sites showed significant inhibition of RNA editing in the mini-gene constract heterologously expressed in HEK 293 cells. The other two ASOs (ASOI and ASOII), that targeted the upstream or downstream regions of ECS which partially overlapped with the ECS, were unable to reduce editing level. With the confirmation of the identity of the ECS that is essential for IQ-domain RNA editing, the $Ca_V1.3$ ECS$^{-/-}$ mouse was generated using whole body knockout strategy.

As observed in our previous study, IQ-domain RNA editing is CNS specific. Therefore, this study mainly focused on the effects of under-edited or unedited $Ca_V1.3$ IQ-domain in the CNS. Evaluation of RNA editing level from the whole brain showed that IQ-domain RNA editing was totally abolished in homozygous $Ca_V1.3$ $ECS^{-/-}$ mice, while under-editing was found in the heterozygous $Ca_V1.3$ $ECS^{+/-}$ mice. Importantly, the expression of Cacna1d at both the RNA and protein levels remained unaffected. Moreover, the other important post-transcriptional modification, alternative splicing at the C-terminus of α1D subunit in $Ca_V1.3$ $ECS^{-/-}$ mice also remained similar to the splicing pattern found in $Ca_V1.3$ WT mice. These basic characterizations of $Ca_V1.3$ $ECS^{-/-}$ mouse at the molecular level suggested that the deletion of ECS in the intronic region specifically eliminated IQ-domain RNA editing without affecting the expression of Cacna1d or alternative splicing at the C-terminus. Thus, the $Ca_V1.3$ $ECS^{-/-}$ mice would be abetter animal model to assess the physiological effects of $Ca_V1.3$ RNA editing.

4.2 Abolished RNA editing in IQ-domain of $Ca_V1.3$ channels in SCN neurons affected spontaneous firing of action potentials and led to disruption of circadian rhythm.

To examine the role of IQ-domain RNA editing in pace-making activity in SCN neurons, the change of editing level with circadian cycle was first investigated. The detected editing level in SCN was higher during the day than at night. This result correlated well with the rhythmic change of firing frequency and Ca^{2+} current. As the edited

$Ca_V1.3$ channel showed slower CDI, elevated RNA editing in the day would result in increased amount of Ca^{2+} influx into the neurons, which might contribute to the higher frequency of spontaneous firing of action potentials. It is also supported by the observations from brain slice recording of $Ca_V1.3$ $ECS^{-/-}$ mice that the firing frequency of action potentials (APs) in SCN neurons was lower than in $Ca_V1.3$ WT mice. Moreover, it is also consistent with previous findings that elimination of RNA editing in $ADAR2^{-/-}$/GluR-$B^{R/R}$ mice led to lower frequency of spontaneous action potential firing in SCN (Huang et al. 2012b).

As it was reported that $Ca_V1.3$ channels were closely coupled to BK channels, the editing level was, however, inversely correlated to the expression level of BK channels as well as the K^+ current (Gilbert R. Pitts et al. 2006, Vaarmann, Gandhi and Abramov 2010). The higher expression level and bigger K^+ current observed at night was thought to hyperpolarize the membrane resulting in the lower firing frequency of spontaneous action potential. It is likely that although the editing level of $Ca_V1.3$ was lower at night, there was still enough Ca^{2+} influx for the activation of BK channels. While during the day, increase of editing in $Ca_V1.3$ channels and decrease of BK channel expression level work in combination to trigger the higher firing frequency of APs. Besides SCN, editing levels of $Ca_V1.3$ channels expressed in the cortex was also evaluated at the 8 time-points over a 24 hour period. The editing levels were maintained at a similar level through-out the day and night.

Rhythmic regulation of $Ca_V1.3$ RNA editing is therefore an inherent feature in the SCN region.

More interestingly, the deletion of IQ domain RNA editing was found to affect circadian regulation. In the running wheel test, $Ca_V1.3$ $ECS^{-/-}$ mice showed 5-fold increase in activity during the day than $Ca_V1.3$ WT mice, indicating disrupted sleep of $Ca_V1.3$ $ECS^{-/-}$ mice. However, this effect was only observed in the day, while during the night, the activities of $Ca_V1.3$ $ECS^{-/-}$ mice and $Ca_V1.3$ WT mice were similar. One possible explanation is that during the day, IQ domain RNA editing level increased to allow more Ca^{2+} influx for the maintenance of pace-making activity. Upon abolishment of editing, due to the faster CDI of the unedited channel, there would be less Ca2+ influx, and thus the firing frequency would be reduced. To determine whether there is a correlation between APs firing frequency and RNA editing, the $Ca_V1.3$ $ECS^{+/-}$ mice will be tested in the future. However, in the night, the normal editing level was relatively low and the neurons in SCN were almost silent. Therefore, upon elimination of editing in $Ca_V1.3$ $ECS^{-/-}$ SCN neurons, the reduced Ca^{2+} influx did not have any significant effect on the pace-making activity nor on the sleep pattern during the night.

The significance of these findings is that the data provide clear evidences that $Ca_V1.3$ RNA editing was involved in regulating pace-making activity in SCN neurons and circadian rhythmic behavior such

as sleep-wake activity. Overall, the regulation of IQ-domain RNA editing and its effect on spontaneous firing and behavior during day and night is summarized in the flow chart (Figure 4.1). To provide further support of this hypothesis, direct measurement of the amount of Ca^{2+} influx into neurons during day and night from the $Ca_V1.3$ $ECS^{-/-}$ and $Ca_V1.3$ WT mice by using Ca^{2+} imaging will be necessary. Furthermore, the detailed behavioral characterization of circadian rhythm in the $Ca_V1.3$ $ECS^{-/-}$ mice such as sleep-wake cycles would be worth studying for better understanding of the effects of deletion of IQ-domain RNA editing on sleep. As Ca^{2+} ions serve as secondary messengers in the cells, the effect of IQ domain RNA editing would not be only on pace-making activity but also on other Ca^{2+}-activated signaling pathways and on gene transcription. The mechanism of how the regulation of editing level could affect the signal output from SCN to other brain regions and controlling the biological clock is still largely unknown.

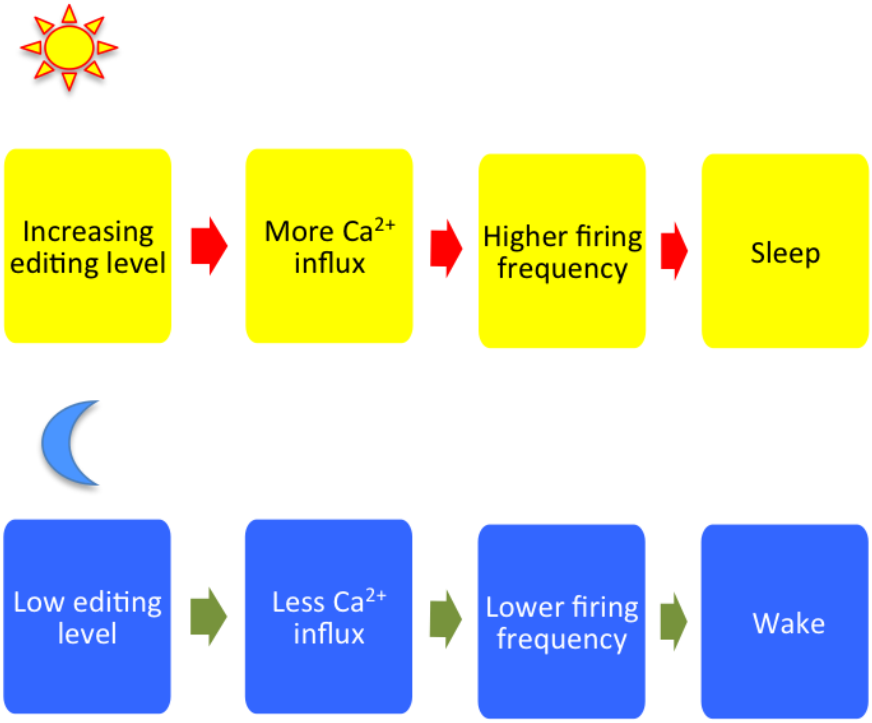

Figure 4.1 Flow chart showing the regulation of RNA editing and its effect on pace-making activity and biologic clock. Upper panel, yellow boxes: the states of editing level, calcium influx, firing frequency and behavior during the day. Lower panel, blue boxes: the states of editing level, calcium influx, firing frequency and behavior during the night.

4.3 IQ-domain RNA editing in SNc up-regulated during aging, while $Ca_V1.3$ $ECS^{-/-}$ mice generally did not exhibit altered motor functions.

The role and modulation of RNA editing in the IQ-domain of $Ca_V1.3$ in aging was also investigated in this study. Increase in editing level during aging was observed in the substantia nigra. It has been reported that the level of editing increased in the first three weeks after birth to reach the adult level and then stably maintained. The developmental change of RNA editing level corresponded to the shift of pace-making

activity from Na^+/HCN-dependent to $Ca_V1.3$-dependent (Chan et al. 2010, Chan et al. 2007).

Our current result showed for the first time that there was a slight increase in editing level during aging especially after the age of 12 month. It provided strong evidence supporting the hypothesis that the growing dependence of Ca^{2+} influx through $Ca_V1.3$ channels would lead to accumulation of oxidative stress and increased vulnerability to mitochondrial toxins could be a cause of neuronal death in Parkinson's disease (Chan et al. 2009, Chan et al. 2010). The increased editing level during aging would lead to more Ca^{2+} influx into the neurons and elevated sensitivity of DA neurons to mitochondrial toxins, while the extra energy consumed for buffering of the increased amount of Ca^{2+} without the help of Ca^{2+} buffering protein calbindin further result in mitochondrial and ER stress (Mosharov et al. 2009, Surmeier et al. 2011b).

One issue is how much of this subtle change of editing level observed in SNc neurons contributes to the oxidative stress. However, it will be very interesting to examine whether $Ca_V1.3$ editing level may be drastically affected in human PD brains. Nevertheless, it is highly possible that there may be other factors involved in the degeneration of DA neurons (Surmeier et al. 2011a). Moreover, it is still unclear whether the increased IQ-domain RNA editing during aging is a cause or consequence of neurodegeneration in SNc. To address this issue,

the $Ca_V1.3$ $ECS^{-/-}$ mouse serves as a good model to assess the effect of deleting RNA editing on the pace-making activity of dopaminergic neurons. Although due to the limitation of time, the electrophysiological analysis of pace-making activity in DA neurons in SNc has not been done yet. Results of behavioral studies testing the motoric function however revealed that generally the $Ca_V1.3$ $ECS^{-/-}$ mice showed similar performance in the tests as the $Ca_V1.3$ WT mice. The increasing latency to fall from accelerating rota-rod during the four testing days observed from both $Ca_V1.3$ $ECS^{-/-}$ and $Ca_V1.3$ WT mice indicated that both of them had the ability of motor learning and balancing on the rota-rod. And they showed similar improvement after four days of testing.

However, the results from the balance beam test seemed to suggest that $Ca_V1.3$ $ECS^{-/-}$ mice had poorer balancing skills than $Ca_V1.3$ WT. As shown by the results from elevated zero maze, $Ca_V1.3$ $ECS^{-/-}$ mice seemed to be more anxious than $Ca_V1.3$ WT mice. One possible explanation for the drastic improvement of time required to cross the beam on the second testing day is that the $Ca_V1.3$ $ECS^{-/-}$ mice on the first testing day were more anxious on the elevated beam. This resulted in them spending more time on the beam on the first day. While on the second day, they were more familiar with the beam and less anxious. Besides, the number of foot slips revealed more about their balancing skill. In contrast to the drastic reduction of time spent to cross the beam, the number of foot slips although decreased during the

three testing days; $Ca_V1.3$ $ECS^{-/-}$ mice had more foot slips when crossing the beam than $Ca_V1.3$ WT mice. Overall, the motoric functions seemed not be grossly affected because of the elimination of IQ-domain RNA editing. Possibly, other behavioral tests are required to show any subtle difference in motoric activities.

Based on our hypothesis, in aged mice, the increased IQ domain RNA editing in $Ca_V1.3$ channels would lead to more Ca^{2+} influx that further contribute to oxidative stress and neurodegeneration. In $Ca_V1.3$ $ECS^{-/-}$ mice there is less Ca^{2+} influx compared to $Ca_V1.3$ WT mice, and this might mimic to some extent a “juvenile” stage that could protect neurons from cell death. Therefore, to test this hypothesis, electrophysiological technique will be used to analyze the spontaneous firing of DA neurons and the underlying Ca^{2+} spikes. One other possible experiment is to test the onset of PD by treatment with mPTP or 6-OHDA, if the hypothesis is correct, the $Ca_V1.3$ $ECS^{-/-}$ mice should gain some degree of protection resulting in delayed PD onset.

For behavioral studies, taking the increase in editing level in SNc during aging which might contribute to the accumulation of oxidative stress into consideration, the differences in motoric functions between $Ca_V1.3$ $ECS^{-/-}$ and $Ca_V1.3$ WT mice might be more obvious when they are aged. The rota-rod and balance beam test could be performed with aged $Ca_V1.3$ $ECS^{-/-}$ and $Ca_V1.3$ WT mice in the future. Mitochondrial toxins could also be used to induce parkinsonian symptoms in both

$Ca_V1.3$ $ECS^{-/-}$ and $Ca_V1.3$ WT mice to answer the question of whether elimination of IQ-domain RNA editing is protective or not.

4.4 $Ca_V1.3$ $ECS^{-/-}$ mice seemed to be more anxious, while no difference in IQ-domain RNA editing was observed in mouse model of depression.

To investigate the role of IQ domain RNA editing in anxiety, elevated zero maze (EZM) test was performed to estimate the anxiety level of $Ca_V1.3$ $ECS^{-/-}$ mice. The $Ca_V1.3$ $ECS^{-/-}$ mice exhibited more anxiety-like behavior on the elevated maze than $Ca_V1.3$ WT mice, as they spent more time in the close arm and traveled less distance during the test. However, in the $Ca_V1.3^{-/-}$ mice, anxiolytic behavior was reported. But similar behavior was also observed in $Cldn14^{-/-}$ mice that were congenitally deaf. Therefore, the anxiolytic behavior was claimed to be contributed by deafness (Busquet et al. 2010). To rule out the influence of hearing on the behavior studies, hearing of $Ca_V1.3$ $ECS^{-/-}$ mice should also be tested in future studies. There is however no reason to suggest $Ca_V1.3$ $ECS^{-/-}$ mice are deaf as it was shown previously that there is no RNA editing of CaV1.3 channels in the cochlea (Huang et al. 2012a). Nevertheless, higher neuronal excitability and impaired LTP observed in amygdala of $Ca_V1.3^{-/-}$ mice still suggested potential roles of $Ca_V1.3$ in anxiety (McKinney et al. 2009).

Moreover, impaired consolidation in $Ca_V1.3^{-/-}$ mice indicated the involvement of $Ca_V1.3$ channels in the consolidation of contextually

conditioned fear (McKinney and Murphy 2006). Thus the effects of altered editing level on anxiety may occur mainly in the amygdala during memory consolidation. One possible explanation may be that there is a compensatory mechanism when the channel is fully deleted. And it is also possible that the compensatory mechanism might enhance the excitability of the neurons trying to make up for the impaired LTP. Furthermore, the impaired consolidation was in line with the impaired LTP in amygdala. However, in $Ca_V1.3$ $ECS^{-/-}$ mice, any compensatory mechanism might be minimal or non-existent as there are unedited $Ca_V1.3$ channels that still function to allow Ca^{2+} influx into the neurons. The reduced amount of Ca^{2+} might result in lower neuronal activity.

But the underlying mechanism of how IQ-domain RNA editing of $Ca_V1.3$ affect anxiety level is still largely unknown. More detailed behavioral studies should be performed. First, more anxiety related tests like light-dark box could be employed to confirm the results observed from EZM. Second, fear conditioning test could also be performed to determine whether consolidation of fear was affected or not in $Ca_V1.3$ $ECS^{-/-}$ mice.

To explore the role of RNA editing in depression, the level of RNA editing of $Ca_V1.3$ was evaluated in depression mouse models in selected brain regions. In the TPH2KI depression mouse model, the editing level was almost the same as it was in the WT mice with normal

behavior. The failure to detect any changes of editing level under depression condition might be due to the type of depression mouse model used in this study. The depression behavior of the TPH2KI mice was mainly due to the deregulation of serotonin synthesis (Jacobsen et al. 2012). Moreover, RNA editing of $Ca_V1.3$ was not affected in this mouse model. However, the antidepressive-like behavior observed in $Ca_V1.3^{-/-}$ mice suggested a role for $Ca_V1.3$ channels in depression (Busquet et al. 2010). Therefore, it would be too hasty to draw the conclusion that IQ-domain RNA editing in $Ca_V1.3$ channel is not involved in depression. To address this issue, depression related behavioral tests such as forced swim test and tail suspension test could be performed with $Ca_V1.3$ $ECS^{-/-}$ mice to see whether elimination of IQ-domain RNA editing would affect depression-like behavior in mice.

Modulation of RNA editing level may become an alternative approach for clinical treatment of mood disorders. Recent study had reported that higher RNA editing level of $5\text{-}HT_{2C}$ receptors was found in suicide victims associated with gene expression and DNA methylation (Di Narzo et al. 2014). More interestingly, in vitro drug screening in SH-SY5Y cells showed that the editing level could be elevated by several drug used in clinical treatment, which might cause depression or suicidal side effects (Cavarec et al. 2013). These studies suggest that RNA editing could be modulated by drug treatment and lead to a related psychiatric event. Results in our study provided new insights

into the underlying mechanisms of mood disorders and might contribute to the development of a new approach for disease treatment.

4.5 Mutation at Y/C editing site in IQ domain had various effects on CDI of $Ca_V1.3$_LF or $Ca_V1.3$_SF splicing variants.

The effect of each RNA editing site and combinations of multiple sites in IQ-domain had been investigated in Huang's previous study. Unlike the other two, although significant level of RNA editing was detected at Y/C site, no obvious change of channel properties was found (Huang et al. 2012a). However, as mentioned in the previous chapter, the editing level at Y/C site was regulated under various physiological conditions. It suggested that RNA editing at Y/C site might have certain effect on the channel.

Previous studies from David Yue's group showed that both isoleucine (I_{1612}/M editing site) to alanine and phenylalanine (F_{1616} downstream next to IQDY) to alanine substitutions in the IQ domain led to reduced CDI and lower affinity of apoCaM binding. But, tyrosine (Y_{1615}) to alanine substitution at the Y/C editing site, removing the tyrosine side chain from protein, resulted in change of neither CDI nor binding affinity of Ca^{2+}/CaM (Bazzazi et al. 2013). However, tyrosine (Y_{1615}) to aspartic acid substitution, mimicking tyrosine phosphorylation, although it did not affect CDI, showed reduced binding affinity to Ca^{2+}/CaM (Ben Johny et al. 2013). These evidences suggested that tyrosine phosphorylation at the Y/C editing site might affect the binding

affinity of Ca^{2+}/CaM. Even though, aspartic acid mimicked the negative charge of tyrosine phosphorylation, the side chains of the two amino acids are significantly different. This might influence the binding affinity as well. The tyrosine (Y_{1615}) to glutamate substitution tested in this study, introduced a negative charge and also maintained a similar side chain structure as tyrosine phosphorylation.

Moreover, it was noticed that the $Ca_V1.3$_LF or $Ca_V1.3$_SF channels have various strength of CDI. With the presence of proximal C-terminal regulatory domain (PCRD) and distant C-terminal regulatory domain (DCRD), $Ca_V1.3$_LF (Ex42 full length channel) exhibit weak CDI as gating of the channel could be modulated by the interaction between DCRD and IQ domain. While $Ca_V1.3$_SF (Ex42a truncated channel), in the absence of DCRD, allow high affinity binding of apoCaM to the IQ-domain to trigger robust CDI (Huang et al. 2013).

Therefore, tyrosine to glutamate substitution was performed in both $Ca_V1.3$_LF and $Ca_V1.3$_SF backbones. The results showed that the strength of CDI and the effect of substitution were indeed different in the two splice variants. In line with previous studies, SF-IQDY and SF-IQDC exhibited similar strength of CDI. The mutant SF-IQDE showed significantly slower CDI as compared to both SF-IQDY and SF-IQDC. The reduction of CDI could possibly be caused by lowered binding affinity to apoCaM or Ca^{2+}/CaM.

As the glutamate substitution mimicked tyrosine phosphorylation, the result suggested that unedited SF-IQDY channel could be phosphorylated at the Y_{1615} site and that would lead to reduced binding affinity of CaM, while the edited SF-IQDC channel maintained high binding affinity to CaM, and thus it exhibited robust CDI. However, in the context of the long-form $Ca_V1.3$ channel, the effect of glutamate substitution was much smaller, and surprisingly, the reduction in CDI observed for edited LF-IQDC and LF-IQDE channels were similar. Interestingly, Y/C editing was only observed in mice and rat, but not in human $Ca_V1.3$ channels (Huang et al. 2012a)

These results indicated that putative tyrosine phosphorylation of the $Ca_V1.3$_LF evoked similar effect on slowing CDI as RNA editing at Y/C site. One possible explanation is that with the presence of DCRD, the gating of $Ca_V1.3$ channel is governed more by the interaction between DCRD and IQ domain and not by the binding of Ca^{2+}/CaM to IQ domain. It is possible that because of different regulatory mechanisms, $Ca_V1.3$_LF channel exhibits slower CDI comparing to $Ca_V1.3$_SF. As such, the reduced CDI of LF-IQDC or LF-IQDE might be due to the altered interaction between DCRD and IQ domain. More importantly, the difference observed between the wild type $Ca_V1.3$-IQDY and mutant $Ca_V1.3$-IQDE in both long-form and short-form splice variants indicated that the wild type channel was not phosphorylated in the HEK 293 cells. However, the phosphatase that catalyzes this tyrosine phosphorylation is still unknown.

Taking the CNS specificity of IQ-domain RNA editing into consideration, it is possible that the phosphatase might express or be activated specifically in the CNS. However, as $Ca_V1.3$ is also expressed in the peripheral tissues, another possibility is that tyrosine phosphorylation could serve as a regulatory mechanism for the gating of $Ca_V1.3$-IQDY channel in peripheral tissues. Results in this study suggest that the Y/C RNA editing might affect CDI through blocking of phosphorylation at the tyrosine site. But the underlying mechanism is still largely unclear, and there are several questions to be answered in future studies.

4.6 Future work

There are several remaining questions to be addressed in future studies. First, all the characterizations discussed above are only in whole brain tissue, other tissue in the CNS had not be investigated yet. Although IQ-domain RNA editing does not occur in peripheral tissues, for a comprehensive characterization, evaluation of Cacna1d expression, IQ-domain RNA editing and alternative splicing should also be performed in those tissues where $Ca_V1.3$ channels are expressed. Second, as $Ca_V1.3$ $ECS^{-/-}$ mice were deleted globally in the CNS, there are certain limitations. First, as the deletion of ECS is full body, in this model it is not able to investigate region-specific effects of IQ-domain RNA editing. Second, all phenotypes observed from $Ca_V1.3$ $ECS^{-/-}$ mice were caused by the global deletion of ECS, therefore, behavioral characterization need to be analyzed carefully.

4.6.1 Characterization of $Ca_V1.3$ $ECS^{-/-}$ mice at RNA and protein level

In this study, $Ca_V1.3$ IQ-domain RNA editing level, Cacna1d transcription level, protein expression level as well as C-terminal alternative splicing have been investigated in the whole brain. The results showed that first, IQ-domain RNA editing was totally abolished in whole brain; second, both *Cacna1d* transcription and protein expression level were the same in $Ca_V1.3$ $ECS^{-/-}$ mice as they were in $Ca_V1.3$ WT mice; third, C-terminal alternative splicing was not affected by the deletion of intronic ECS.

However, as IQ-domain RNA editing occurs specifically in the CNS, the editing level, transcription level, protein expression and C-terminal splicing should also be investigated in the spinal cord. Moreover, for a more comprehensive characterization, the transcription level, protein expression and C-terminal alternative splicing would need to be checked in peripheral tissues where $Ca_V1.3$ channels are expressed. For characterization at the RNA level, an alternative method could be to use RNA sequencing technology to investigate the transcriptome profile. As Ca^{2+} is one of the most important second messenger molecule that triggers diverse downstream signal pathways, it would help to uncover changes in transcriptome profiles between $Ca_V1.3$ $ECS^{-/-}$ mice and $Ca_V1.3$ WT mice, and to provide evidence for understanding the molecular mechanism underlying pace-making activity and behavioral outcomes. However, for protein expression,

besides whole cell lysates, surface expression would be more informative on function. Surface biotinylation could be used to isolate $Ca_V1.3$ channels from cell membrane for the comparison of the amount of functional $Ca_V1.3$ channels on the cell membrane.

4.6.2 Characterization of pace-making activity of neurons in SCN and SNc

As $Ca_V1.3$ channels play an important role in the pace-making activity of neurons in SCN and SNc, the effect of IQ-domain RNA editing on spontaneous firing of action potential is worth studying. The preliminary results showed that the firing frequency of SCN neurons was lower in $Ca_V1.3$ $ECS^{-/-}$ mice. However, the underlying Ca^{2+} spike and detailed analysis of action potential have yet been characterized. The lower firing frequency would suggest that less Ca^{2+} influx into the neurons was a result of elimination of IQ-domain RNA editing. Electrophysiological method could be used to perform whole-cell patch clamp to record the spontaneous firing of action potentials from both SCN and SNc nerons. The GCaMP6 transgenic mice (Jaxson's lab) could be used as an alternative method to monitor Ca^{2+} levels.

The transgenic mice contain Ca^{2+} sensor eGFP-calmodulin fusion protein that can be induced by a tetracycline transactivator. By crossing the GCaMP6 mice with $Ca_V1.3$ $ECS^{-/-}$ mice or $Ca_V1.3$ WT mice, expression of GCaMP6 would enable visualization of Ca^{2+} dynamics and changes that could act as a surrogate of neuronal activity *in vivo*. It

would provide indirect evidence of changes of neuronal activity in various brain regions such as SCN, SNc, hippocampus, amygdala and prefrontal cortex in $Ca_V1.3$ $ECS^{-/-}$ mice. The correlation between neuronal activity in different brain regions and behavior outcomes in various behavioral studies would be helpful for understanding physiological roles of IQ-domain RNA editing of the $Ca_V1.3$ channels.

4.6.3 Phenotyping of $Ca_V1.3$ $ECS^{-/-}$ mice

Several behavioral tests had been performed in this study with homologous $Ca_V1.3$ $ECS^{-/-}$ mice and their WT littermates. Higher level of anxiety, disrupted circadian rhythm and slight deficiency in balancing ability were observed from $Ca_V1.3$ $ECS^{-/-}$ mice. However, these preliminary results were obtained from $Ca_V1.3$ $ECS^{-/-}$ mice with one generation of backcrossing. The genetic background of $Ca_V1.3$ $ECS^{-/-}$ mice is mixed with C57BL/6, SV129 (ES cells) and FVB (β-Actin CRE mice). Therefore, backcrossing into C57BL/6 background to at lease 6-10 generations would be necessary. More comprehensive and detailed phenotyping would be performed with such backcrossed $Ca_V1.3$ $ECS^{-/-}$ and $Ca_V1.3$ WT mice.

First, the general health condition of the $Ca_V1.3$ $ECS^{-/-}$ mice would be investigated. It will include basic testing of hearing and vision functions, body weight and metabolism. As hearing and vision functions would affect the outcome of many behavioral tests, it is important and necessary to know whether the $Ca_V1.3$ $ECS^{-/-}$ mice have any

deficiencies in hearing and vision. The $Ca_V1.3$ $ECS^{-/-}$ mice will be aged to determine their longevity and to assess whether they would develop any age-related diseases. Their body weights will be recorded at different ages. Their metabolism rates would also be examined by housing them in metabolic cages.

Second, anxiety and depression related behavioral tests would be performed. For testing of anxiety level, besides elevated zero maze, light-dark box could also be used to test the anxiety level of mice. As observed in EZM, the $Ca_V1.3$ $ECS^{-/-}$ mice seemed to be quite comfortable with normal lighting conditions, thus in order to provide an anxious environment, the lighting conditions in the box might need to be adjusted. For the testing of depression level, several tests can be used: for example, tail suspension test and forced swimming tests. As each behavioral test has various confounding factors, it would be more meaningful to perform more than one test for each aspect of behavioral assessment.

Third, for a more detailed analysis of motor coordination, besides rota-rod test and balance beam test, gait analysis will be performed to investigate motor functions of the $Ca_V1.3$ $ECS^{-/-}$ mice. In the rota-rod test, there was not much difference observed for their performances on the rota-rod between $Ca_V1.3$ $ECS^{-/-}$ and $Ca_V1.3$ WT mice. However, in the balance beam test, the longer time $Ca_V1.3$ $ECS^{-/-}$ mice spent on crossing the beam was only observed on the first day of test, and they

performed almost as well as $Ca_V1.3$ WT mice on the following two days. The number of foot slips when crossing the beam suggested that the $Ca_V1.3$ $ECS^{-/-}$ mice seemed to have a slight deficiency in balance.

Therefore, in future studies the number of mice used in the behavioral test will be increased to obtain more convincing results, and gait analysis should be performed to analyze detailed motor coordination to determine whether the $Ca_V1.3$ $ECS^{-/-}$ mice may have motor deficiency. Moreover, as mentioned previously in this study, the level of RNA editing in the IQ domain increased during aging, the effect of deletion IQ-domain RNA editing might show up in aging. It could be possible that the differences in motor function between $Ca_V1.3$ $ECS^{-/-}$ and $Ca_V1.3$ WT mice might show up in aged mice. Therefore, the same tests will need to be performed with aged $Ca_V1.3$ $ECS^{-/-}$ and $Ca_V1.3$ WT mice to examine what the effect IQ-domain RNA editing may have on motoric functions in aged mice.

Fourth, the results of the running wheel test indicated disrupted circadian rhythm of $Ca_V1.3$ $ECS^{-/-}$ mice. Further characterization of circadian rhythmic pattern of the $Ca_V1.3$ $ECS^{-/-}$ mice would be essential. In the running wheel test, the $Ca_V1.3$ $ECS^{-/-}$ mice seemed to be more active than $Ca_V1.3$ WT mice during the day when they were supposed to be sleeping. Therefore, characterization of the sleep-wake cycle would help to address the question of whether the high activity level during the day was caused by disrupted sleep or not. The sleep-wake

cycle will be first recorded under 12hr-light-dark (LD) cycles, and then the circadian rhythmic pattern under 12hr-dark-dark (DD) condition will be recorded. The results would reveal first whether the circadian rhythm could be synchronized by LD cycle; second whether $Ca_V1.3$ $ECS^{-/-}$ mice exhibit free run circadian rhythmic pattern under DD cycles or the circadian rhythmic pattern would be disrupted. This study would provide direct evidence suggesting the role of IQ-domain RNA editing in the regulation of circadian rhythm.

At last, as suggested by our previous study, $Ca_V1.3$ channels seemed to be involved in the consolidation of contextual fear conditioning (McKinney and Murphy 2006). Fear conditioning could test learning and memory of $Ca_V1.3$ $ECS^{-/-}$ mice. The three phases of acquisition, consolidation and extinction will all be tested to determine the effect of abolished IQ-domain RNA editing on conditioned fear.

Before performing fear conditioning, vision and hearing of $Ca_V1.3$ $ECS^{-/-}$ mice should be tested as mentioned above. The choice of whether to perform contextual fear conditioning or auditory fear conditioning will be based on the results of the hearing and vision tests of the $Ca_V1.3$ $ECS^{-/-}$ mice. If $Ca_V1.3$ $ECS^{-/-}$ mice exhibit any deficiencies in hearing or vision, it would affect the related behavioral outcomes observed from fear conditioning test. Because either visual or auditory stimulus are involved in the test, for instance, if hearing of

the $Ca_V1.3$ $ECS^{-/-}$ mice was impaired, then visual stimulus will be used in the test to investigate contextual conditioned fear.

Besides, if the vision of $Ca_V1.3$ $ECS^{-/-}$ mice were not impaired, Morris water maze will also be conducted to test learning and memory. $Ca_V1.3$ $ECS^{-/-}$ and $Ca_V1.3$ WT mice will be trained to find the hidden platform in the water maze by guide from the space cues. These studies will help to determine the role of IQ-domain RNA editing in learning and memory.

The phenotyping tests mentioned above will also be performed with $Ca_V1.3$ $ECS^{+/-}$ mice. Because as presented in chapter 3, the editing level detected in $Ca_V1.3$ $ECS^{+/-}$ mice is half of the level in $Ca_V1.3$ WT mice. It would be interesting to investigate whether the effects of IQ-domain RNA editing on behavioral outcome is does-dependent or not.

4.6.4 Investigation of tyrosine phosphorylation at Y/C editing site

The substituted $Ca_V1.3$ channel mimicking phosphorylation at Y/C editing site showed reduced CDI, suggesting that tyrosine phosphorylation might also regulate CDI probably by altering the binding affinity of CaM or DCRD respectively in $Ca_V1.3$_SF or $Ca_V1.3$_LF. To investigate the role of RNA editing at Y/C site, first, as the tyrosine phosphorylation was predicted by computational program, it would need to be confirmed and it is important to know the distribution as to whether it occurs specifically in CNS or peripheral

tissues or both. Second, to verify the assumption that the reduced CDI is caused by altered binding between IQ domain and its regulatory effector, binding affinity between IQ domain and DCRD in $Ca_V1.3$_LF or IQ domain in $Ca_V1.3$_SF and CaM will be evaluated. Third, the tyrosine phosphatase will need to be identified. Furthermore, regulation of this tyrosine phosphorylation would be another question to be answered. Moreover, the regulation of tyrosine phosphorylation may also be associated with CNS specificity of IQ-domain RNA editing.

4.7 Conclusion

The $Ca_V1.3$ channels are widely expressed in the brain, though at a much lower level than the paralogous $Ca_V1.2$ channels. Nevertheless, dysfunction of the $Ca_V1.3$ channels has been associated with or implicated in mood disorders, Parkinson's disease and circadian regulation. In this study, it is the first time IQ domain RNA editing level was evaluated under various physiological and pathological conditions. The circadian rhythmic modulation of editing level detected in SCN strongly suggested the important roles of IQ domain RNA editing in modulating pace making activity of the SCN neurons. The increase in $Ca_V1.3$ RNA editing in SN during aging might indicate the contribution of RNA editing to the accumulation of oxidative stress in DA neurons that could contribute to neuronal death.

The generation of the $Ca_V1.3$ $ECS^{-/-}$ mice provided an animal model to investigate the functional role of RNA editing. It helped to reveal the

effects of deleting RNA editing on electrophysiological as well as the behavioral levels. The elimination of IQ-domain RNA editing resulted in lower firing frequency of pace making activity in SCN neurons and further disrupted the circadian rhythm activity of these mice. Moreover, the anxiety level was also observed in the $Ca_V1.3$ $ECS^{-/-}$ mice, and this is likely an amygdala-effect.

Our recent work on the pharmacological inhibition of $Ca_V1.3$ channel provided a new piece of evidence for drug discovery for therapeutic treatments (Huang et al. 2014). The results in this study may contribute new insights into how calcium channel could be pharmacologically manipulated for therapeutic benefits and build up the link between post-transcriptional modification of calcium channel and biological behaviors.

Bibliography:

Ashani, K. & B. L. Bass (2012) Mechanistic insights into editing-site specificity of ADARs. PNAS.

Baig, S. M., A. Koschak, A. Lieb, M. Gebhart, C. Dafinger, G. Nurnberg, A. Ali, I. Ahmad, M. J. Sinnegger-Brauns, N. Brandt, J. Engel, M. E. Mangoni, M. Farooq, H. U. Khan, P. Nurnberg, J. Striessnig & H. J. Bolz (2011) Loss of Ca(v)1.3 (CACNA1D) function in a human channelopathy with bradycardia and congenital deafness. Nature Neuroscience, 14, 77-84.

Bazzazi, H., M. Ben Johny, P. J. Adams, T. W. Soong & D. T. Yue (2013) Continuously tunable Ca(2+) regulation of RNA-edited CaV1.3 channels. Cell Rep, 5, 367-77.

Beaulieu, J. M., X. Zhang, R. M. Rodriguiz, T. D. Sotnikova, M. J. Cools, W. C. Wetsel, R. R. Gainetdinov & M. G. Caron (2008) Role of GSK3 beta in behavioral abnormalities induced by serotonin deficiency. Proc Natl Acad Sci U S A, 105, 1333-8.

Belle, M. D., C. O. Diekman, D. B. Forger & H. D. Piggins (2009) Daily electrical silencing in the mammalian circadian clock. Science, 326, 281-4.

Ben Johny, M., P. S. Yang, H. Bazzazi & D. T. Yue (2013) Dynamic switching of calmodulin interactions underlies Ca2+ regulation of CaV1.3 channels. Nat Commun, 4, 1717.

Berg, K. A., Cropper, J. D., Niswender, C. M., Sanders & E. Bush, Emeson, R. B., and Clarke, W. P (2001) RNA-editing of the 5-HT2C receptor alters agonist-receptor-effector coupling specicity. Br. J. Pharmacol, 134.

Bhalla, T., J. J. Rosenthal, M. Holmgren & R. Reenan (2004) Control of human potassium channel inactivation by editing of a small mRNA hairpin. Nat Struct Mol Biol, 11, 950-6.

Brooks, S. P. & S. B. Dunnett (2009) Tests to assess motor phenotype in mice: a user's guide. Nat Rev Neurosci, 10, 519-29.

Busquet, P., N. Khoi Nguyen, E. Schmid, N. Tanimoto, M. W. Seeliger, T. Ben-Yosef, F. Mizuno, A. Akopian, J. Striessnig & N.

Singewald (2009) CaV1.3 L-type Ca2+ channels modulate depression-like behaviour in mice independent of deaf phenotype. The International Journal of Neuropsychopharmacology, 13, 499.

Busquet, P., N. K. Nguyen, E. Schmid, N. Tanimoto, M. W. Seeliger, T. Ben-Yosef, F. Mizuno, A. Akopian, J. Striessnig & N. Singewald (2010) CaV1.3 L-type Ca2+ channels modulate depression-like behaviour in mice independent of deaf phenotype. Int J Neuropsychopharmacol, 13, 499-513.

Catterall, W. A. (2000) Structure and regulation of voltage-gated Ca2+ channels. Annu. Rev. Cell Dev. Biol., 16.

Cavarec, L., L. Vincent, C. Le Borgne, C. Plusquellec, N. Ollivier, P. Normandie-Levi, F. Allemand, N. Salvetat, E. Mathieu-Dupas, F. Molina, D. Weissmann & J. F. Pujol (2013) In vitro screening for drug-induced depression and/or suicidal adverse effects: a new toxicogenomic assay based on CE-SSCP analysis of HTR2C mRNA editing in SH-SY5Y cells. Neurotox Res, 23, 49-62.

Chan, C. S., T. S. Gertler & D. J. Surmeier (2009) Calcium homeostasis, selective vulnerability and Parkinson's disease. Trends in Neurosciences, 32, 249-256.

--- (2010) A molecular basis for the increased vulnerability of substantia nigra dopamine neurons in aging and Parkinson's disease. Movement Disorders, 25, S63-S70.

Chan, C. S., J. N. Guzman, E. Ilijic, J. N. Mercer, C. Rick, T. Tkatch, G. E. Meredith & D. J. Surmeier (2007) ‘Rejuvenation’ protects neurons in mouse models of Parkinson’s disease. Nature, 447, 1081-1086.

Colwell, C. S. (2011) Linking neural activity and molecular oscillations in the SCN. Nat Rev Neurosci, 12, 553-69.

Daniel, C., M. T. Venø, Y. Ekdahl, J. Kjems & M. O. hman (2012) A distant cis acting intronic element induces site-selective RNA editing. Nucleic Acids Res, 1.

Daniel, C., H. Wahlstedt, J. Ohlson, P. Bjork & M. Ohman (2011) Adenosine-to-inosine RNA editing affects trafficking of the

gamma-aminobutyric acid type A (GABA(A)) receptor. J Biol Chem, 286, 2031-40.

Decher, N., A. K. Streit, M. Rapedius, M. F. Netter, S. Marzian, P. Ehling, G. Schlichthorl, T. Craan, V. Renigunta, A. Kohler, R. C. Dodel, R. A. Navarro-Polanco, R. Preisig-Muller, G. Klebe, T. Budde, T. Baukrowitz & J. Daut (2010) RNA editing modulates the binding of drugs and highly unsaturated fatty acids to the open pore of Kv potassium channels. EMBO J, 29, 2101-13.

Di Narzo, A. F., A. Kozlenkov, P. Roussos, K. Hao, Y. Hurd, D. A. Lewis, E. Sibille, L. J. Siever, E. Koonin & S. Dracheva (2014) A unique gene expression signature associated with serotonin 2C receptor RNA editing in the prefrontal cortex and altered in suicide. Hum Mol Genet.

Gilbert R. Pitts, Hidenobu Ohta & D. G. McMahon (2006) <Daily rhythmicity of large-conductance Ca2+ -activated K+ currents in suprachiasmatic nucleus neurons..pdf>. brain research, 1071, 9.

Goldberg, J. A., J. N. Guzman, C. M. Estep, E. Ilijic, J. Kondapalli, J. Sanchez-Padilla & D. J. Surmeier (2012) Calcium entry induces mitochondrial oxidant stress in vagal neurons at risk in Parkinson's disease. Nature Neuroscience, 15, 1414-21.

Gurevich, I., Hadassah Tamir, Victoria Arango, Andrew J. Dwork, J. John Mann & C. Schmauss (2002) Altered Editing of Serotonin 2C Receptor Pre-mRNA in the Prefrontal Cortex of Depressed Suicide Victims. Neuron, 34.

Huang, H., C. Y. Ng, D. Yu, J. Zhai, Y. Lam & T. W. Soong (2014) Modest CaV1.342-selective inhibition by compound 8 is b-subunit dependent. Nat Commun.

Huang, H., B. Z. Tan, Y. Shen, J. Tao, F. Jiang, Y. Y. Sung, C. K. Ng, M. Raida, G. Kohr, M. Higuchi, H. Fatemi-Shariatpanahi, B. Harden, D. T. Yue & T. W. Soong (2012a) RNA editing of the IQ domain in Ca(v)1.3 channels modulates their Ca(2)(+)-dependent inactivation. Neuron, 73, 304-16.

Huang, H., Bao Z. Tan, Y. Shen, J. Tao, F. Jiang, Ying Y. Sung, Choon K. Ng, M. Raida, G. Köhr, M. Higuchi, H. Fatemi-

Shariatpanahi, B. Harden, David T. Yue & Tuck W. Soong (2012b) RNA Editing of the IQ Domain in Cav1.3 Channels Modulates Their Ca2+-Dependent Inactivation. Neuron, 73, 304-316.

Huang, H., D. Yu & T. W. Soong (2013) C-terminal alternative splicing of CaV1.3 channels distinctively modulates their dihydropyridine sensitivity. Mol Pharmacol, 84, 643-53.

Hurley, M. J., B. Brandon, S. M. Gentleman & D. T. Dexter (2013) Parkinson's disease is associated with altered expression of CaV1 channels and calcium-binding proteins. Brain, 136, 2077-97.

Jackson, A. C., G. L. Yao & B. P. Bean (2004) Mechanism of spontaneous firing in dorsomedial suprachiasmatic nucleus neurons. The Journal of neuroscience : the official journal of the Society for Neuroscience, 24, 7985-98.

Jacobsen, J. P., I. O. Medvedev & M. G. Caron (2012) The 5-HT deficiency theory of depression: perspectives from a naturalistic 5-HT deficiency model, the tryptophan hydroxylase 2Arg439His knockin mouse. Philos Trans R Soc Lond B Biol Sci, 367, 2444-59.

Kent, J. & A. L. Meredith (2008) BK channels regulate spontaneous action potential rhythmicity in the suprachiasmatic nucleus. PLoS One, 3, e3884.

Mangoni, M. E., B. Couette, E. Bourinet, J. Platzer, D. Reimer, J. Striessnig & J. Nargeot (2003) Functional role of L-type Cav1.3 Ca2+ channels in cardiac pacemaker activity. Proc Natl Acad Sci U S A, 100, 5543-8.

Marcantoni, A., P. Baldelli, J. M. Hernandez-Guijo, V. Comunanza, V. Carabelli & E. Carbone (2007) L-type calcium channels in adrenal chromaffin cells: role in pace-making and secretion. Cell Calcium, 42, 397-408.

McKinney, B. C. & G. G. Murphy (2006) The L-Type voltage-gated calcium channel Cav1.3 mediates consolidation, but not

extinction, of contextually conditioned fear in mice. Learn Mem, 13, 584-9.

McKinney, B. C., W. Sze, B. Lee & G. G. Murphy (2009) Impaired long-term potentiation and enhanced neuronal excitability in the amygdala of Ca(V)1.3 knockout mice. Neurobiol Learn Mem, 92, 519-28.

Meredith, A. L., S. W. Wiler, B. H. Miller, J. S. Takahashi, A. A. Fodor, N. F. Ruby & R. W. Aldrich (2006) BK calcium-activated potassium channels regulate circadian behavioral rhythms and pacemaker output. Nat Neurosci, 9, 1041-9.

Miyoko, H., Frank N. Single, Martin Kohler, Bernd Sommer, Rolf Sprengel & P. H. Seeburg (1993) RNA Editing of AMPA Receptor Subunit GluR-9- A Base-Paired Intron-Exon Structure Determines Position and Efficiency. Cell 75.

Mosharov, E. V., K. E. Larsen, E. Kanter, K. A. Phillips, K. Wilson, Y. Schmitz, D. E. Krantz, K. Kobayashi, R. H. Edwards & D. Sulzer (2009) Interplay between cytosolic dopamine, calcium, and alpha-synuclein causes selective death of substantia nigra neurons. Neuron, 62, 218-29.

Namkung, Y., N. Skrypnyk, M.-J. Jeong, T. Lee, M.-S. Lee, H.-L. Kim, H. Chin, P.-G. Suh, S.-S. Kim & H.-S. Shin (2001) Requirement for the L-type Ca2+ channel α1D subunit in postnatal pancreatic β cell generation. Journal of Clinical Investigation, 108, 1015-1022.

Ohlson, J., J. S. Pedersen, D. Haussler & M. Ohman (2007) Editing modifies the GABA(A) receptor subunit alpha3. Rna, 13, 698-703.

Pennartz, C. M. A., M. T. G. D. Jeu, A. M. S. Geurtsen, A. A. Sluiter & M. L. H. J. Hermes (1998) Electrophysiological and morphological heterogeneity of neurons in slices of rat suprachiasmatic nucleus. Journal of Physiology, 506.

Pennartz, C. M. A., M. T. G. d. Jeu，, N. P. A. Bos，, J. Schaap， & A. M. S. Geurtsen (2002) Diurnal modulation of pacemaker

potentials and calcium current in the mammalian circadian clock. NATURE, 416.

Peterson, B. Z., DeMaria CD, Adelman JP & Y. DT. (1999) Calmodulin Is the Ca21 Sensor for Ca21-Dependent Inactivation of L-Type Calcium Channels. Neuron, 22, 549-558.

Platzer, J., J. Engel, A. Schrott-Fischer, K. Stephan, S. Bova, H. Chen, H. Zheng & J. Striessnig (2000) Congenital deafness and sinoatrial node dysfunction in mice lacking class D L-type Ca2+ channels. Cell, 102.

Rula, E. Y., A. H. Lagrange, M. M. Jacobs, N. Hu, R. L. Macdonald & R. B. Emeson (2008) Developmental modulation of GABA(A) receptor function by RNA editing. The Journal of neuroscience : the official journal of the Society for Neuroscience, 28, 6196-201.

Seeburg, P. H., M. Higuchi & R. Sprengel (1998) RNA editing of brain glutamate receptor channels- mechanism and physiology. Brain Research Reviews, 26, 217-229.

Streit, A. K. & N. Decher (2011) A-to-I RNA editing modulates the pharmacology of neuronal ion channels and receptors. Biochemistry (Mosc), 76, 890-9.

Streit, A. K., C. Derst, S. Wegner, U. Heinemann, R. K. Zahn & N. Decher (2011) RNA editing of Kv1.1 channels may account for reduced ictogenic potential of 4-aminopyridine in chronic epileptic rats. Epilepsia, 52, 645-8.

Surmeier, D. J., J. N. Guzman, J. Sanchez-Padilla & J. A. Goldberg (2011a) The Origins of Oxidant Stress in Parkinson's Disease and Therapeutic Strategies. ANTIOXIDANTS & REDOX SIGNALING, 14.

Surmeier, D. J., Jaime N. Guzman, Javier Sanchez-Padilla & P. T. Schumacker (2011b) The role of calcium and mitochondrial oxidant stress in the loss of substantia nigra pars compacta dopaminergic neurons in Parkinson's disease. neuroscience, 198.

Tan, B. Z., F. Jiang, M. Y. Tan, D. Yu, H. Huang, Y. Shen & T. W. Soong (2011) Functional characterization of alternative splicing in the C

terminus of L-type CaV1.3 channels. J Biol Chem, 286, 42725-35.

Vaarmann, A., S. Gandhi & A. Y. Abramov (2010) Dopamine Induces Ca2+ Signaling in Astrocytes through Reactive Oxygen Species Generated by Monoamine Oxidase. Journal of Biological Chemistry, 285, 25018-25023.

Vandael, D. H., A. Marcantoni, S. Mahapatra, A. Caro, P. Ruth, A. Zuccotti, M. Knipper & E. Carbone (2010) <Cav1.3 and BK Channels for Timing and Regulating Cell Firing.pdf>. molecular neurobiology, 42, 14.

Vandael, D. H., A. Zuccotti, J. Striessnig & E. Carbone (2012) Ca(V)1.3-driven SK channel activation regulates pacemaking and spike frequency adaptation in mouse chromaffin cells. J Neurosci, 32, 16345-59.

Wright, A. & B. Vissel (2012) The essential role of AMPA receptor GluR2 subunit RNA editing in the normal and diseased brain. frontiers in molecular neuroscience, 5, 13.

Xu, W. & D. Lipscombe (2001) Neuronal CaV1.3 1 L-Type Channels Activate at Relatively Hyperpolarized Membrane Potentials and Are Incompletely Inhibited by Dihydropyridines. The journal of neuroscience, 21.

Yukio, K., H. S. Kyoko Ito, Hitoshi Aizawa, Ichiro Kanazawa & S. Kwak (2004) RNA editing and death of motor neurons. nature, 427.

Zhang, H., Y. Fu, C. Altier, J. Platzer, D. J. Surmeier & I. Bezprozvanny (2006) Ca1.2 and CaV1.3 neuronal L-type calcium channels: differential targeting and signaling to pCREB. The European journal of neuroscience, 23, 2297-310.

Zhang, H., A. Maximov, Y. Fu, F. Xu, T. S. Tang, T. Tkatch, D. J. Surmeier & I. Bezprozvanny (2005a) Association of CaV1.3 L-type calcium channels with Shank. The Journal of neuroscience : the official journal of the Society for Neuroscience, 25, 1037-49.

Zhang, X., R. R. Gainetdinov, J. M. Beaulieu, T. D. Sotnikova, L. H. Burch, R. B. Williams, D. A. Schwartz, K. R. Krishnan & M. G. Caron (2005b) Loss-of-function mutation in tryptophan

hydroxylase-2 identified in unipolar major depression. Neuron, 45, 11-6.

Zhang, Z., Y. He, D. Tuteja, D. Xu, V. Timofeyev, Q. Zhang, K. A. Glatter, Y. Xu, H. S. Shin, R. Low & N. Chiamvimonvat (2005c) Functional roles of Cav1.3(alpha1D) calcium channels in atria: insights gained from gene-targeted null mutant mice. Circulation, 112, 1936-44.